Organic carbon in Mediterranean sapropels: the interplay between anoxia, productivity and clay mineral association

Thesis submitted in accordance with the requirements of the University of Adelaide for an Honours Degree in Geology

Robyn Jean Williamson

November 2013

THE UNIVERSITY of ADELAIDE

TITLE

Mechanisms of organic carbon preservation on Mediterranean sapropels: The interplay between anoxia, productivity, and clay mineral association.

RUNNING TITLE

Clay mineral, anoxia, productivity

ABSTRACT

Despite numerous studies conducted within the Mediterranean basin to understand the timing and climatic influences governing the formation of organic rich sedimentary layers, sapropels, a conclusion regarding the mechanisms behind the enrichment and preservation of the organic carbon (OC) within the sapropels remains elusive. As such, a significant flaw within our understanding of biogeochemical processes that influence the climate and oxygenation of the Earth's oceans and atmosphere exists. Current literature is dominated by two hypotheses which attempt to explain the enrichment and preservation of OC with no consensus between the two schools of thought. One of which highlights oxygen depleted, anoxic water conditions as a factor while the second relies upon increased productivity within the water column. As such, this study proposes a third hypothesis which states that an increase in organic matter (OM) preservation may be related to the increased presence of the high surface area mineral, smectite (Wehausen & Brumsack 1999, Foucault & Melieres 2000) at the time of sapropel formation. This study investigates the interaction between OM and the mineral matrix within core sample from the Ocean Drilling Program (ODP) Leg 160 site 967 using multiple methods including: SEM imaging, XRD analysis, EGME 'free surface' mineral area (MSA) testing, and geochemical testing for total organic carbon (TOC) and $CaCO_3$ content. From these methods, we falsified the hypothesis that MSA is a dominant factor in the preservation of OM by the lack of correlation present between MSA and TOC. Instead, results obtained during this study provide new evidence supporting the model presented by Kemp et al. (1999) which hypothesises siliceous productivity is the mechanism controlling OM preservation within sapropels. As such, this study presents Kemp's model of productivity as the preferred method of OC enrichment and preservation within the Mediterranean Basin, and subsequently furthers our understanding of the biogeochemical processes governed by OC. However, continued study of these OC rich sediments is required to better understand the burial and preservation of OC within this region.

KEYWORDS

Mediterranean, Sapropel, Anoxia, Productivity, Clay Mineral Association, Organic Carbon Preservation

Contents

LIST OF FIGURES AND TABLES

INTRODUCTION

The burial of organic carbon (OC) is one of the most fundamental biogeochemical processes on Earth, influencing temperature and oxygenation of the oceans and atmosphere (Hedges & Keil 1995, Burdige 2007). Greater than 95% of OC preserved at the surface of the Earth is buried in continental margin sediments (Hedges & Keil 1995), but this represents only a small fraction (<0.5%) of marine primary production (Burdige 2007). Anomalous concentrations of organic matter within specific intervals of the geologic record (e.g. the Cretaceous Oceanic Anoxic Events) imply that the carbon burial efficiency is variable, and is likely influenced by changing environmental conditions. However, the mechanisms controlling the formation of organic-rich marine sediments, especially ancient deposits such as the Cretaceous black shales, remain poorly understood with no consensus within the scientific community at present (Hedges & Keil 1995, Burdige 2007).

Modern analogues can be used to better understand the mode of formation of ancient deposits (Tyson 2005). An example of a recent analogue for OC enrichment found in Cretaceous black shales is the cyclical organic-rich deposits in the Mediterranean basin known as sapropels (Rohling 1994), which are interbedded with organic-lean marls. Due to its restricted nature and size, the Mediterranean basin can be considered a natural laboratory, where changes in environmental/climatic conditions evoke strong responses in basinal conditions. The Mediterranean is a particularly well-suited site for the study of the relative impacts of climatic, oceanographic and terrestrial influences on OC burial in marine sediments. Initially discovered in the eastern Mediterranean basin (EMB) in the 1960s and later in the western Mediterranean basin (WMB) in the 1990s, sapropels

are a characteristic feature of Mediterranean sediments dating back to at least the Pliocene (Bouloubassi *et al.* 1999).

Sapropels are brown to black sediments, often occurring in laminated beds with marls. Sapropels are noted for their high OC contents, which range between 2-30% total organic carbon (TOC) (Hilgen 1991, Bouloubassi *et al.* 1999, Struck *et al.* 2001). Enriched in trace elements, biogenic Ba, smectite, chlorite, illite, Fe and S, they are in marked contrast to their organic-lean interbedded counterpart (Foucault & Melieres 2000, Nijenhius & De-Lange 2000). The marls, often described as carbonaceous ooze, are defined by <1% TOC content and an abundance of aeolian derived sediments of kaolinite, palygorskite, feldspars and quartz (Foucault & Melieres 2000). The notable differences between the marls and the sapropels can be attributed to their different depositional environments and sediment source regions.

At present the Mediterranean Basin is ogliotrophic, nutrient poor, with a temperate climate (Struck *et al.* 2001), similar to the conditions in which marls are deposited. However, sapropels are known to be deposited under more humid conditions associated with increased fluvial activity, which are linked to precession minima and insolation maxima with a 21,000 year periodicity (Rossignol-Strick 1982, 1983, 1985, Rohling 1994, Foucault & Melieres 2000, Rohling *et al.* 2002). With this orbitally-forced change in climate, evidence for increased nutrient inputs to the Mediterranean, lower surface water salinities and switches in the dominant sediment source are observed (Rossignol-Strick 1982, Emeis *et al.* 1998).

This orbitally-forced switch in climate is considered the trigger for sapropel deposition in the two main schools of thought on the mechanisms of sapropels formation: increased productivity and anoxia. With increased nutrient availability to the system, one school of thought considers an increase in primary productivity with higher settling fluxes of OC to the sediment-water interface as the main cause of OC enrichment in sapropels. The second school of thought considers the enhanced preservation of organic carbon (OC) under oxygen depleted conditions to be the main control on sapropel formation, reasoning that increased fluvial discharge and a decrease in surface salinity during more humid intervals leads to stratification and oxygen-depleted bottom waters.

Evidence of oxygen deficiency (anoxia) within the Mediterranean Sea has been widely documented within sapropels, especially of Pliocene age (Passier *et al.* 1999, Nijenhius & De-Lange 2000, Struck *et al.* 2001). Evidence for anoxia includes the enrichment of redox-sensitive trace elements (Wehausen & Brumsack 1999, Nijenhius & De-Lange 2000, Struck *et al.* 2001), the presence of isorenieratene (a biomarker indicative of euxinic conditions in the photic zone) (Passier *et al.* 1999), and the absence of benthic macrofauna as indicated by the presence of lamination in sapropels (Nijenhius & De-Lange 2000). However, it is unlikely that anoxia alone can account for organic carbon enrichment in sapropels. An increase of up to 2 orders of magnitude in TOC from background marls (<0.5% TOC) to sapropels (30% TOC) has commonly been documented in the Mediterranean Sea (Emeis *et al.* 1998, Cramp & O'Sullivan 1999, Nijenhius & De-Lange 2000, Struck *et al.* 2001). However, enhanced preservation due to oxygen depletion alone can only explain a 5 to 6 times increase in OC relative to oxic conditions (Tyson 2005). Therefore, to explain the substantial increase of 2 orders of

magnitude, other factors in the promotion of organic matter preservation must be assessed.

Increased primary productivity at the time of sapropel deposition may account for part of the OC enrichment observed. Increased primary productivity and export flux of OC is indicated by palaeoproductivity reconstructions using the proxy biogenic-barium (Ba) (Wehausen & Brumsack 1999, Nijenhius & De-Lange 2000, Weldeab *et al.* 2003), increased biogenic silicon (Kemp *et al.* 1999) comparable to high productivity oceanic sites, and low stable isotope ratios of $\delta^{15}N$ and $\delta^{13}C$ (Calvert *et al.* 1992, Struck *et al.* 2001) as well as microfaunal assemblages characteristic of higher productivity settings (Kemp *et al.* 1999). Higher primary production could lead to increased fluxes of OC to the seafloor and a higher biological oxygen demand as sinking OM is mineralized in the water column, which could result in oxygen depletion and anoxia in deep waters (Calvert *et al.* 1992). Thus, it has been argued that productivity is the sole controller of sapropel formation, providing both the increased OM and the environmental conditions, such as anoxia, needed for formation (Calvert *et al.* 1992). However, the Mediterranean is usually an oligotrophic, nutrient-poor, environment and the increase in productivity needed for sapropel formation requires an increased supply of nutrients into the system (Struck *et al.* 2001). Such increases in the nutrient budget might result from extra riverine input into the system or upwelling of nutrients from deep water.

An alternative pathway to OC enrichment has recently been identified, involving the continentally and climatically controlled supply of high surface area detrital clay minerals with a preservative effect on OC (Kennedy & Wagner 2011). Mineral surface

area (MSA) controlled preservation of OC has the potential to be significant because detrital clay minerals comprise > 60% of continental margin sediments. MSA is determined by the abundance of specific clay minerals with high surface area (Chamley 1989, Kennedy & Wagner 2011). Preservation of OM in association with clay mineral surface may provide an alternative explanation for OC enrichment in sapropels. Recent work by Keil *et al.* (1994), Mayer (1994), Kennedy *et al.* (2002), and Kennedy and Wagner (2011) have shown that a positive relationship between MSA and TOC exists within both OC-rich modern and ancient sediments. The available mineral surface area is a function of the abundance of weathering-derived clays, specifically smectite (Kennedy & Wagner 2011). Known as a swelling clay, smectite has a hydratable interlayer in which OM can be preserved from degradation (Kennedy & Wagner 2011). With higher proportions of smectites in sapropels relative to marls, this mechanism could be the cause of OC enrichment in the Mediterranean Sea.

This study assessed the relationship between OM and the mineral matrix in Pliocene sediments from ODP leg 160 site 967 (Figure 1) to test the hypothesis that increased clay mineral surface area corresponds to an increase in the preservation of OC and the formation of sapropels. A multi-scale approach was employed, including both bulk scale mineralogical and geochemical characterization of the samples, as well as high resolution scanning electron microscope (SEM) back scatter electron (BSE) imaging of OM – mineral associations.

GEOLOGICAL SETTING/BACKGROUND

The Messinian salinity crisis affected the Mediterranean Sea with the closing of the paleo-Mediterranean from the Atlantic Ocean via the Betic passage and Rifian corridor

by tectonic uplift associated with the collision of the African and Eurasian plates between 5.96±0.02 Ma and 5.33Ma (Benson *et al.* 1991, Loget & Van Den Driessche 2006). This closing led to extensive fluvial channel incision by both major and minor channels and deposited an extensive evaporitic deposit (Loget & Van Den Driessche 2006). Flooding of the Mediterranean Basin through the strait of Gibraltar via an erosive stream 5.33 Ma marked the end of the Messinian salinity crisis and the re-establishment of open marine conditions (Loget & Van Den Driessche 2006, Garcia-Castellanos *et al.* 2009). Since the opening of the Strait of Gibraltar 5.33 Ma, no change in the physical geography and oceanography has occurred within the Mediterranean Basin.

Although physically the basin has not changed since 5.33Ma, climatic influences have cyclically changed the depositional environment within the basin since its return to open marine settings (Rossignol-Strick 1982, 1983, 1985, Rohling 1994, Rohling *et al.* 2002). First noted by Rossignol-Strick (1982), a strong correlation between precession minima and insolation maxima over Africa has been noted to coincide with the onset of sapropel formation. The precessional and insolation changes have been found to influence the African climate, creating a humid environment and increasing fresh water supply to the Mediterranean basin (Petit-Marie & Riser 1981, Rossignol-Strick 1982, 1983, 1985, Claussen *et al.* 1999).

Earth's orbital parameters: eccentricity, obliquity and precession, influence the distribution and proportion of incoming solar radiation and therefore climate (Imbrie & Imbrie 1980). These parameters reach a maximum influence every 100,000 years,

41,000 years and 21,000 years respectively (Imbrie & Imbrie 1980). Rossignol-Strick (1983), showed that increased solar insolation associated with precession minima affected the North African continent, creating an intensification and northward migration of the African monsoon.

With the intensification and northward migration of the African monsoon, changes in vegetation and fluvial activity across Northern Africa occurred (Rossignol-Strick 1982, 1983, 1985, Rohling 1994, Rohling *et al.* 2002). Pollen data record changes from arid deserts to open grassland and shrubland, while higher slopes within mountainous regions record broader leafed trees (Rossignol-Strick 1982, Claussen *et al.* 1999). Fluvial activity peaked in Northern Africa at the same time with the presence of local lakes demonstrated by fresh water fish, molluscs, ostracods and charophytes (Petit-Marie & Riser 1981) as well as increased rainfall to the catchment areas of the Nile (Rossignol-Strick 1982).

An increase to the freshwater budget along the northern borderlands of Africa not only affects Africa but also the Mediterranean basin (Rossignol-Strick 1982, 1983, 1985, Rohling 1994). Previous studies conducted on planktonic foraminifera within the sapropels show a decrease in $\delta^{18}O$ relating to a decrease in salinity at the time of sapropel formation (Emeis *et al.* 1998). A drop in salinity at the time of sapropel formation can be accounted for by an increase in freshwater input from fluvial channels in the northern borderlands of Africa and the Nile (Rossignol-Strick 1982, 1983, Emeis *et al.* 1998, Rohling *et al.* 2002).

Circulation within the Mediterranean is dependent on the increase of salinity of surface water to the east creating a density gradient strong enough to create convection downwards to form intermediate and deep water formation (Bethoux 1993, Rohling 1994). At present the Mediterranean basin is divided by the strait of Sicily into two main sub-basins; Western Mediterranean basin (WMB) and Eastern Mediterranean basin (EMB) (Figure 2; (Bethoux 1993, Rohling 1994)). The WMB and EMB are both divided into further sub basins, with the western basin composed of the Alboran, Balearic and Tyrrhenian Seas and the eastern basin composed of the Aegean, Levantine and Adriatic Seas (Figure 2) (Cramp & O'Sullivan 1999).

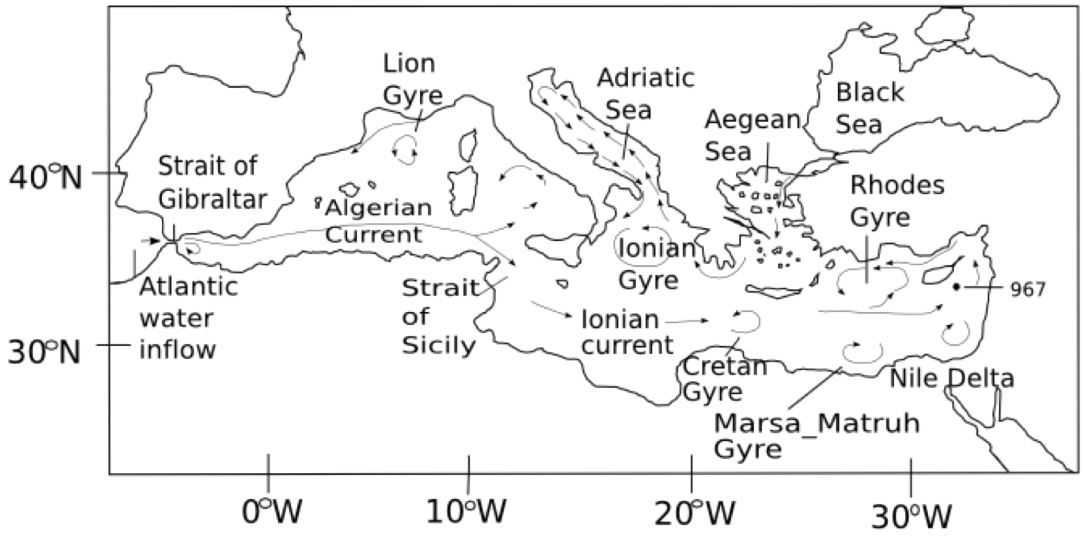

Figure 1: Overview of the Mediterranean Basin showing sub-basins, currents, gyres and the sample location of site 967 drafted and adapted from Rohling *et al.* (2009).

Circulation within the Mediterranean basin follows an anti-estuarine flow; surface water flows in from the Atlantic spreading eastwards from the Strait of Gibraltar while flowing sub-surface Mediterranean intermediate water (MIW) flows outwards to the

Atlantic (Figure 3; Rohling (1994)). MIW is composed mainly of Levantine intermediate water (LIW), formed when surface water flows east from the Atlantic, increasing in salinity due to evaporation loss (Bethoux 1993, Rohling 1994). When surface water reaches the eastern most part of the basin, salinity is increased by evaporation and creates a greater density in the water, which sinks downwards to create intermediate water which is warm and dense (LIW) (Figure 3; (Bethoux 1993, Rohling 1994)). As the LIW travels westwards over the strait of Sicily to the western basin, it mixes with the regional intermediate waters creating the MIW (Bethoux 1993, Rohling 1994).

Deep-water formation in the Mediterranean occurs in the WMB and EMB separately (Figure 3). In the EMB formation of the deep water occurs in both the Adriatic and Aegean Seas when cold winter winds cool the surface waters in these regions creating downward convection and ventilation into deep-water masses (Bethoux 1993, Rohling 1994). In the WMB a similar formation occurs when cool winter winds create downwards convection of MIW in the Gulf of Lions into deep-water (Bethoux 1993, Rohling 1994). The formation and circulation of these different water masses within the Mediterranean are highly sensitive to shifts in the hydrological budget (Myers 2002).

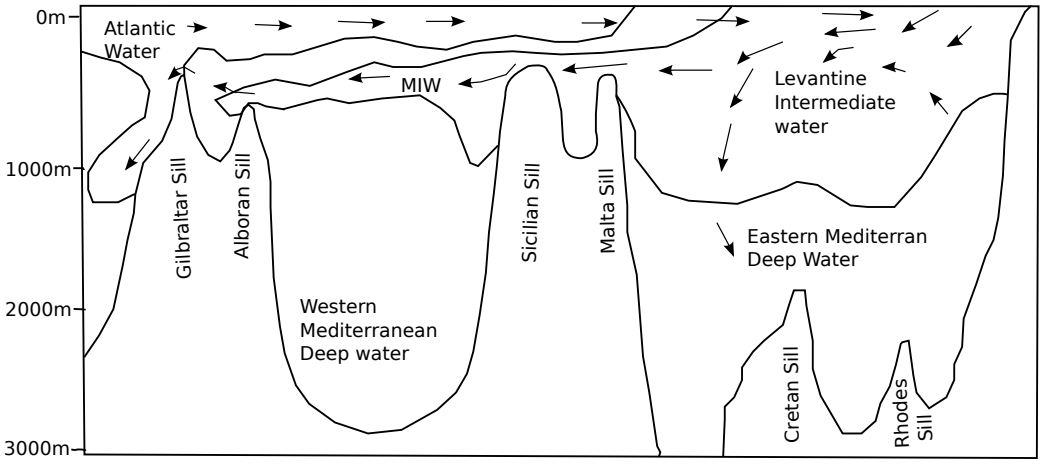

Figure 2: Cross-section of the hydrology of the Mediterranean Basin, showing places of formation of the different water masses and their pathways across the basin drafted and adapted from Rohling *et al.* (2009).

Decreases in the salinity budget of the Mediterranean due to increased freshwater input to the surface layer, can cause changes to the circulation and formation of the different water masses in the Mediterranean Sea (Myers 2002). Myers (2002) showed that modest decreases in salinity of only 8% can result in the inhibition of the intermediate and deep-water formation. Such an inhibition in the formation of these water masses could result in decreased convection of oxygen to the deep-water profile and slowly cause anoxia through oxygen depletion (Emeis *et al.* 1998, Myers 2002). Previously Emeis *et al.* (1998) studied salinity and sea surface temperatures in the Mediterranean from alkenone records, revealing a lag in salinity decrease of surface water between 600-1500yr before the onset of sapropel formation, establishing a frame work for oxygen depleted bottom waters.

Increased freshwater inputs to the Mediterranean could also explain possible sources of nutrients. The model provided by Myers (2002) explained that a possible nutrient trap

could be created by widespread circulation changes due to the input of freshwater in to the EMB. This nutrient trap is the product of intermediate water formation in the Adriatic Sea (AIW) instead of the formation of LIW interrupting normal downward convection patterns. The AIW moves both east to the EMB and west over the Strait of Sicily trapping nutrients in the EMB when normal circulation would circulate nutirents westwards out of the Mediterranean basin.

Increased freshwater influx, creating possible nutrient traps and changes in the hydrology of the Mediterranean, is integral to the onset of sapropel formation (Emeis *et al.* 1998, Cramp & O'Sullivan 1999, Nijenhius & De-Lange 2000, Struck *et al.* 2001, Rohling *et al.* 2002) . Two competing hypotheses for the OC enrichment in the Mediterranean are anoxia or increased productivity. The anoxia hypothesis uses the change in hydrology created from increased freshwater to account for oxygen water depletion within deep waters. Increased productivity uses the increased nutrient supply brought by the fluvial runoff to explain increases in primary production and greater OC fluxes to the seafloor.

With less than 1% of primary production surviving to be preserved in the sedimentary record few areas exist in which enrichment occurs (Burdige 2007). Muller and Suess (1979) who studied marine sediments and the comparison of primary production rates and preservation, recorded that only a fraction of organic carbon produced is preserved within the sedimentary record. Primary production created in the photic zone must travel before it reaches its final resting place at the bottom of the sea floor. As it settles OC is lost through oxidation and degradation (Murat & Got 2000, Tyson 2005).

Emerson (1985) stated that carbon contents in marine sediments is simply a function of oxygen concentration and its ability to penetrate sediments and oxidize carbon.

Oxygen depletion (anoxia) within the Mediterranean Sea at the time of sapropel formation is well evidenced (Passier *et al.* 1999, Nijenhius & De-Lange 2000, Struck *et al.* 2001). However, the large up to 2 orders of magnitude increase experienced between marls (<0.5%) and sapropels (30%) cannot be entirely explained by anoxia. Tyson (2005) recently stated that only a 5 to 6 times OC enrichment within sediments can be accounted for by oxygen depletion (anoxia) compared to oxic conditions. One possible explanation to the substantial two orders of magnitude increase could be from an increase in primary productivity at the time of sapropel formation.

Increases in primary production are known to account for higher carbon fluxes of OM (Tyson 2005) to the sea floor and have been heavily implicated as a contributing factor in the formation of sapropels (Calvert *et al.* 1992, Nijenhius & De-Lange 2000, Struck *et al.* 2001, Weldeab *et al.* 2003) . With a higher rate of primary production present at the time of sapropel formation, increases of OC and higher utilization of oxygen from biological demand as OM is remineralized in the water column could result in oxygen depletion in the water column (Calvert *et al.* 1992). Thus, increased primary production may be both the source of OM and the controller of formation. However, the time lag between decreased surface water salinity to the onset of sapropel formation (600-1500 years) is too prolonged to be the result of productivity controlling oxygen depletion (Emeis *et al.* 1998).

However, evidence still exists for both hypotheses with some models provided from studies combining the two to create an environment in which both anoxia and productivity create an interplay in the formation of sapropels (Cramp & O'Sullivan 1999, Kemp *et al.* 1999, Nijenhius & De-Lange 2000, Rohling *et al.* 2002). Kemp *et al.* (1999) presented such a model in which both anoxia and productivity interacted in the formation of sapropels. In their model, differences between silica productivity during spring blooms and summer created two different laminae expressed in the Holocene sapropel S5 (Kemp *et al.* 1999). Laminae switched between the mixed diatom assemblage of the spring bloom and rhizolsonid diatom-mats of the summer production (Kemp *et al.* 1999). Rhizosolenid mats are sensitive to water agitation as they cycle from depth where they receive nutrients to surface waters where they photosynthesize (Kemp *et al.* 1999). Summer stratification due to increased freshwater from the African monsoon would inhibit intermediate and deep-water formation in the basin, creating an ideal environment for rhizosolenid mats to exist (Emeis *et al.* 1998, Kemp *et al.* 1999, Myers 2002). However when agitation of the water column from strong fall/winter winds occurs a 'fall-dump' event of OM would be created (Kemp *et al.* 1999). Although this model provides a scenario for each hypothesis, contention still is present within the scientific community.

A third hypothesis involves OC enrichment in sediments due to the high surface area of detrital clay minerals in continental margins (Kennedy & Wagner 2011). A positive correlation between the mineral surface area of sediments and TOC values has been established recently within both OC-rich modern and ancient sediments (Keil *et al.* 1994, Mayer 1994, Kennedy *et al.* 2002, Kennedy & Wagner 2011). Surface area,

within these studies was found to be dependent on the abundance of weathering-derived clays, specifically smectite (Kennedy & Wagner 2011). Known as a swelling clay, smectite has an hydratable interlayer in which OM can be preserved from degradation, providing a mechanism for preservation of OC (Kennedy & Wagner 2011).

Switches in sediment sources are noted between marls and sapropels that coincide with the intensification and northward migration of the African monsoon (Wehausen & Brumsack 1999, Foucault & Melieres 2000). Specifically, the switch in source sediment is seen as a switch from aeolian sourced clay dominance (kaolinite and palygorskite) in marls to a fluvial sourced clay dominance (smectite, illite and chlorite) in sapropels. Aeolian sourced palygorskite and kaolinite are characteristic clay minerals of Saharan dust while smectite, illite and chlorite are fluvially sourced clay minerals from mountainous regions around the Mediterranean (Figure 3) (Foucault & Melieres 2000). During humid conditions, vegetation changes to northern Africa reduce aeolian dust mobility, limiting its contribution to the Mediterranean detrital budget (Claussen *et al.* 1999). Increased precipitation to mountainous regions, would account for increased weathering, increasing the migration of smectite, illite and chlorite to the Mediterranean (Stanely & Wingerath 1996, Foucault & Melieres 2000). As such, humid conditions and increased precipitation to Africa and surrounding Mediterranean can account for the known switch seen in clay minerals between the sediments (marls vs sapropel).

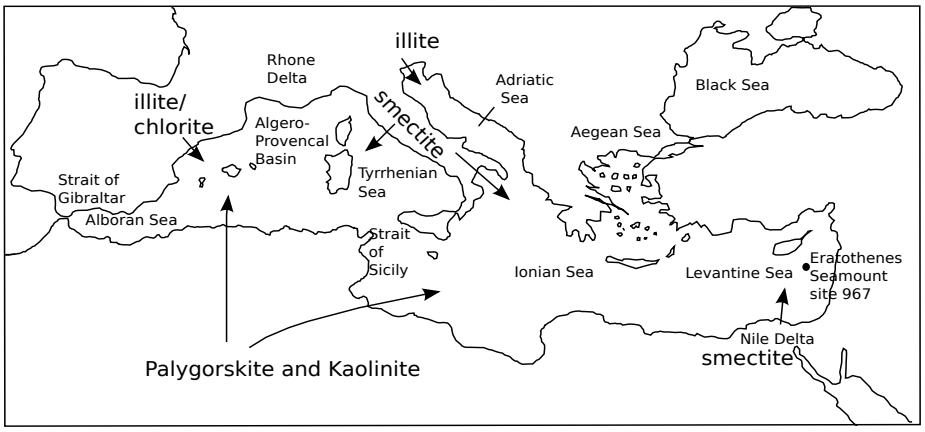

Figure 3: Distribution of clay mineral sources around the Mediterranean Basin showing dominant clay source locations within reference to study site ODP 967, adapted and drafted from Foucault and Melieres (2000).

Furthermore, the Nile and African northern borderlands are chief fluvial contributors to the Mediterranean Basin at times of increased precipitation (Rohling *et al.* 2002). The Nile, sourced from the Ethiopian Highlands, is a known source of smectite and suspended sediments from the Nile sediment load show a dominance in the clay fraction (Adamson *et al.* 1980, Stanely & Wingerath 1996, Foucault & Melieres 2000). With higher proportions of smectite recorded in sapropel samples relative to marls, an alternative explanation for OC enrichment in sapropels could be reliant on the mechanistic preservation relationship between smectite and OM.

METHODS

Sample Collection and Subsampling:

Three sapropel cycles of Pliocene age were sampled from the Ocean Drilling Program (ODP) Leg 160 Site 967 at cm-scale resolution (Figure 4). Site 967 is located between the collisional zone of the Eratosthenes Seamount and the subduction zone of the

Eurasian plate boundary at Cyprus within the Levantine basin (Figure1) (Robertson 1998), at a water depth of 2555m. The three sapropels sampled correspond to insolation cycles (i-cycles) i-280, i-282 and i-284 (Emeis *et al.* 2000), with astronomically timed ages of 2.943, 2.965 and 2.989 Ma respectively. 94 samples were collected in total, at 1-cm scale in sapropels and 5-cm spacings in marls. To capture the depositional environment of each sample geochemical and mineralogical testing has been conducted as well as an assessment of physical characteristics. 51 samples which were received sufficiently intact were subsampled for SEM imaging of OM distribution and association with mineral phases. The remaining sample material was milled using a ring mill to pass through a 250µm sieve prior to geochemical and mineralogical testing.

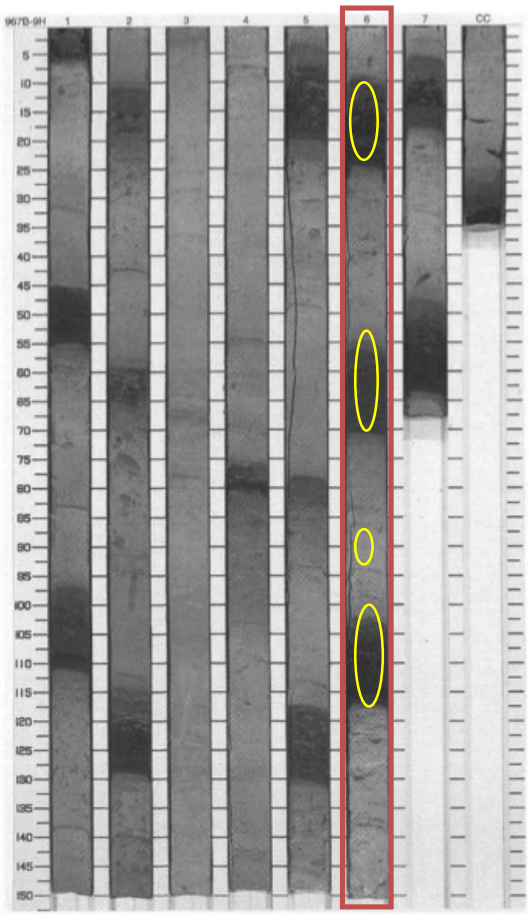

Figure 4: Core photo of ODP leg 160, core 967B-9H (Emeis *et al.* 1996). The area outlined in red shows section 6 of the core which was subsampled for this study, corresponding to three sapropel cycles of Pliocene age correlated to insolation cycles i-280, i-282 and i-284, with astronomically timed ages 2.943, 2.965 and 2.989 ma respectively (Emeis *et al.* 2000). The yellow ovals mark locations of samples imaged using scanning electron microscopy. This sampled interval was retrieved from 79.3 meters below sea floor.

Geochemistry:

Total carbon (TC) and total nitrogen (TN) concentrations were determined using a Perkin-Elmer CHN analyser (detailed methods in appendix C). Inorganic carbon (IC) was determined using the pressure calcimeter method of Sherrod *et al.* (2002) (detailed method in Appendix B). Total organic carbon (TOC) content was calculated by subtracting IC from TOC (TOC= TC-IC).

Sediment mineral surface area (MSA) was measured using the 'free surface' Ethylene Glycol Monoethyl Ether (EGME) method (Kennedy & Wagner 2011) which measures total MSA as EGME is able to access and sorb to both external and internal surface areas of expandable clay minerals. Approximately 0.5g of each sample was catio-exchanged with 1N CaCl solution and rinsed of excess salt. As part of the method 30 standards were run with the batch of 94 samples. The standards comprised of two smectite clay standards (Texas montmorillonite, STx-1 and Na-montmorillonite, Swy-2), an illite standard (Imt-1) and 2 inhouse laboratory shale standards (Mancos unweathered and Mancos weathered). All samples were weighed into glass vials and dried for 48 hours at 110°C before being soaked in 1 ml of EGME and placed in a vacuum chamber with excess EGME and granular $CaCl_2$. All samples were weighed before entering the chamber and reweighed periodically until a stable weight was obtained, at which point a monolayer coverage of EGME on the sample surfaces was assumed.The equilibrated mass of EGME (MG) per g sample was then converted to mineral surface area using a conversion factor of 3.2 (Kennedy & Wagner 2011). Analysis of the standards revealed that Mancos weathered and Mancos unweathered mixed clay both showed average surface area values of 217.43 ± 2.314 m^2g^{-1} and 208.804 ± 2.762m^2g^{-1} respectively. While analysis of illite, IMt-1, Texas

montmorillonite, STx-1 and Na-montmorillonite Swy-2 from the Clay mineral society showed surface area values of 127.916 ± 1.495 m^2g^{-1}, 760.857 ± 2.677 m^2g^{-1} and 722.415 ± 3.853 m^2g^{-1} respectively, therefore showing good reproducibility.

MSA was remeasured in all samples with >1% TOC after organic matter removal with a pH adjusted (pH9.5) solution of sodium hypochlorite (Appendix G) (Anderson 1963). The samples were left in 10ml sodium hypochlorite solution at 80°C for 1 hour before being centrifuged and rinsed. This process was repeated 4 times, with an additional 3 rinses with DIW being performed after the last repetition before the samples were left in the oven at 40°C to dry. Mineral surface area was recorded after the organic matter removal to test whether the mineral surface area values measured originally were impacted by interaction of EGME with OM.

Imaging:

Thirteen subsamples were imaged by SEM using an FEI Quanta 450 in BSEI to establish the relationship between OM and minerals present with each sample (detailed method explained in Appendix D). The samples were chosen based on their location within the core (Figure 1). Imaged samples included two samples chosen at the interface between the sapropel and marl, 2 marls and 9 sapropel samples, 3 from each sapropel. Samples were mounted on SEM stubs with Araldite perpendicular to the plane of bedding and polished using both sandpaper and the Fishione 1060 SEM mill for 8 hours to obtain a flat polished surface free of mechanical damage before being coated with platinum for imaging.

Samples selected for imaging had varying degrees of bioturbation (major, minor or absent) to determine if bioturbation affected how OM was associated in the mineral

matrix. Bioturbation was judged on how each sample appeared under optical microscopy or ODP photos when the samples were not sufficiently large or did not arrive intact. Major bioturbation is defined as no observed lamination with evidence of burrowing and homogenous sediments. Minor is defined as a sample with preserved lamination with minor evidence of burrowing. Absent is defined as preserved lamination with no indication of burrowing.

Clay mineralogy:

Clay mineralogy of six samples from within sapropel i-284 and the marl segments surrounding it was determined by x-ray diffraction of oriented preparations of the clay size fraction. Organic matter and carbonates were removed prior to separation of the clay size fraction. The removal involved a water bath at a temperature of 90°C with carbonates removed first using a pH 5 1M sodium acetate/acidic acid buffer to rinse the samples 3 times before then rinsing the samples with a pH adjusted solution of sodium hypochlorite of 9.5pH to remove the organic matter present within the samples (adapted from (Moore & Reynolds)). The <2 μm fraction of the samples was then separated by centrifugation after ultrasonic dispersal of the samples, and placed in the oven for drying before a known quantity of sample was used to prepare the orientated preparations for XRD analysis.

Samples were scanned between a 2θ range of 3.5° and 45° with a step size of 0.05° at 1.5 seconds a step using a Bruker D8 Advance XRD with a Cu source. Each sample was scanned after several different treatments (air dried, heat treatments at 400°C, and Ethylene Glycol coated) and clay minerals were identified using the criteria of Poppe *et al.* (2001) (detailed method in Appendix F).

OBSERVATIONS AND RESULTS

Geochemical Testing

TOC AND CARBONATE RESULTS:

TOC varies between <0.1% and 14. 7% with a range of <0.1% -0.7% in marls and 1-14.7% in sapropels (Table 1 and Figure 5). Sapropel i-280 has the highest TOC content with a maximum of 14.7% and average of 7.4%. The oldest sapropel, i-284, records TOC values as high as 10.2% and an average of 6.7%. Lowest TOC values are recorded with in the middle sapropel, i-282, with a maximum of 7.2% and an average of 4.3%.

Table 1: **Maximum, minimum and average results for sapropel cycles i-280 to i-284 and interbedded marls, comparing total organic carbon (TOC), TOC on a $CaCO_3$ free basis, $CaCO_3$ contents, EGME measured surface area, and $CaCO_3$ free surface area, and surface area and $CaCO_3$ free surface area of sapropels where organic matter (OM) was removed. i-280 records the highest surface areas, and TOC values, but has the lowest $CaCO_3$ contents. Note that measured surface areas of sapropels i-280 to i-284 after OM removal is similar to marl surface areas.**

		TOC (%)	$CaCO_3$ free TOC (%)	$CaCO_3$ (%)	Surface area (m^2g^{-1})	Surface area (m^2g^{-1})-$CaCO_3$ free	Surface area after Om removal (m^2g^{-1})	OM removed surface area (m^2g^{-1})-$CaCO_3$ free
i-280	min	1.1	2.2	0.1	231.3	316.4	185.1	203.2
	max	14.7	15.8	48.7	513.3	515.9	332.5	385.2
	average	7.4	8.8	19.2	327.8	409.5	240.2	302.1
i-282	min	1	1.7	33.4	195	408.2	143.4	316
	max	7.2	11.5	59.3	303.5	479.4	254.4	416.6
	average	4.3	7.6	42.6	257.6	449.5	206.8	359.5
i-284	min	1.3	2.1	35.4	164.4	383.4	146.2	294.5
	max	10.2	19.4	57.1	286.5	494.6	220.5	345.5
	average	6.7	11.8	42.5	255.5	445.3	182.6	317.7
marls	min	0.02	0.04	20.7	143.1	242.5	N/A	N/A
	max	0.7	1.4	62.2	251.8	430.6	N/A	N/A
	average	0.2	0.4	48	195.3	376.4	N/A	N/A

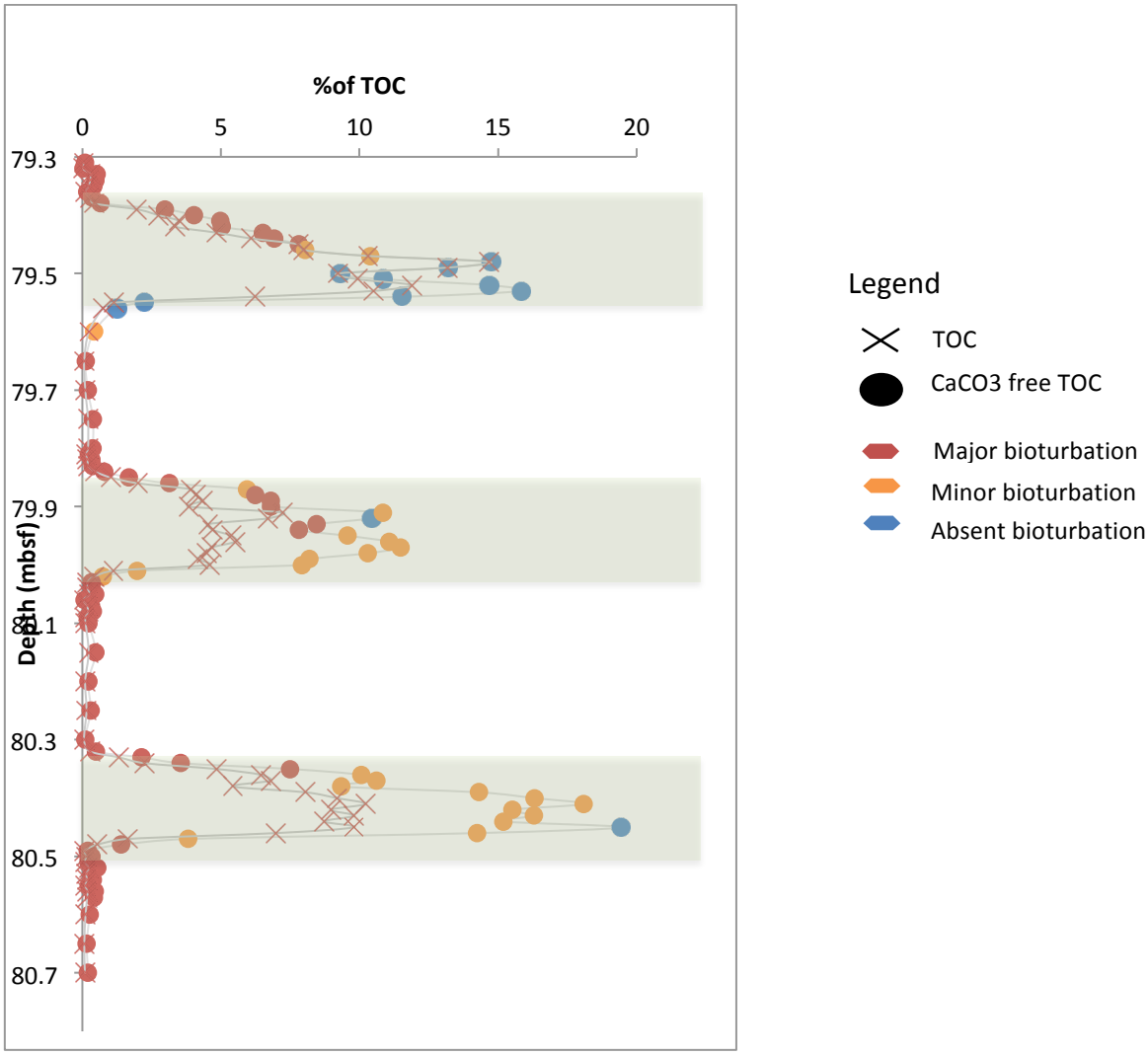

Figure 5:Total organic carbon (TOC) content (cross) and $CaCO_3$ free TOC values (circles) plotted against depth in meters below sea floor (mbsf) for sapropel cycles i-280 – i-284 (grey boxes). Before $CaCO_3$ correction, the highest recorded TOC values were present in i-280, but on a $CaCO_3$ free basis, i-284 records the highest TOC values. Symbol colours refer to the degrees of bioturbation within the samples. Red is classified as major bioturbation where there is no observed lamination, with evidence of burrowing and homogenous sediments in the sample. Yellow refers to minor bioturbation in which there is some preserved lamination and minor evidence of burrowing present in the sample. Blue refers to absent bioturbation in which there is preserved lamination and no indication of burrowing.

$CaCO_3$ concentrations within the core range from a maximum of 62.2% to a minimum of 0.1% (Table 1), with lowest concentrations within the youngest sapropel, i-280, which also shows the largest variations in $CaCO_3$%, with a sharp drop from a maximum

of 48.7% to a minimum of 0.1%, (Figure 6). Both i-282 and i-284 have similar ranges for $CaCO_3$ content between 59.3% and 33.4%.

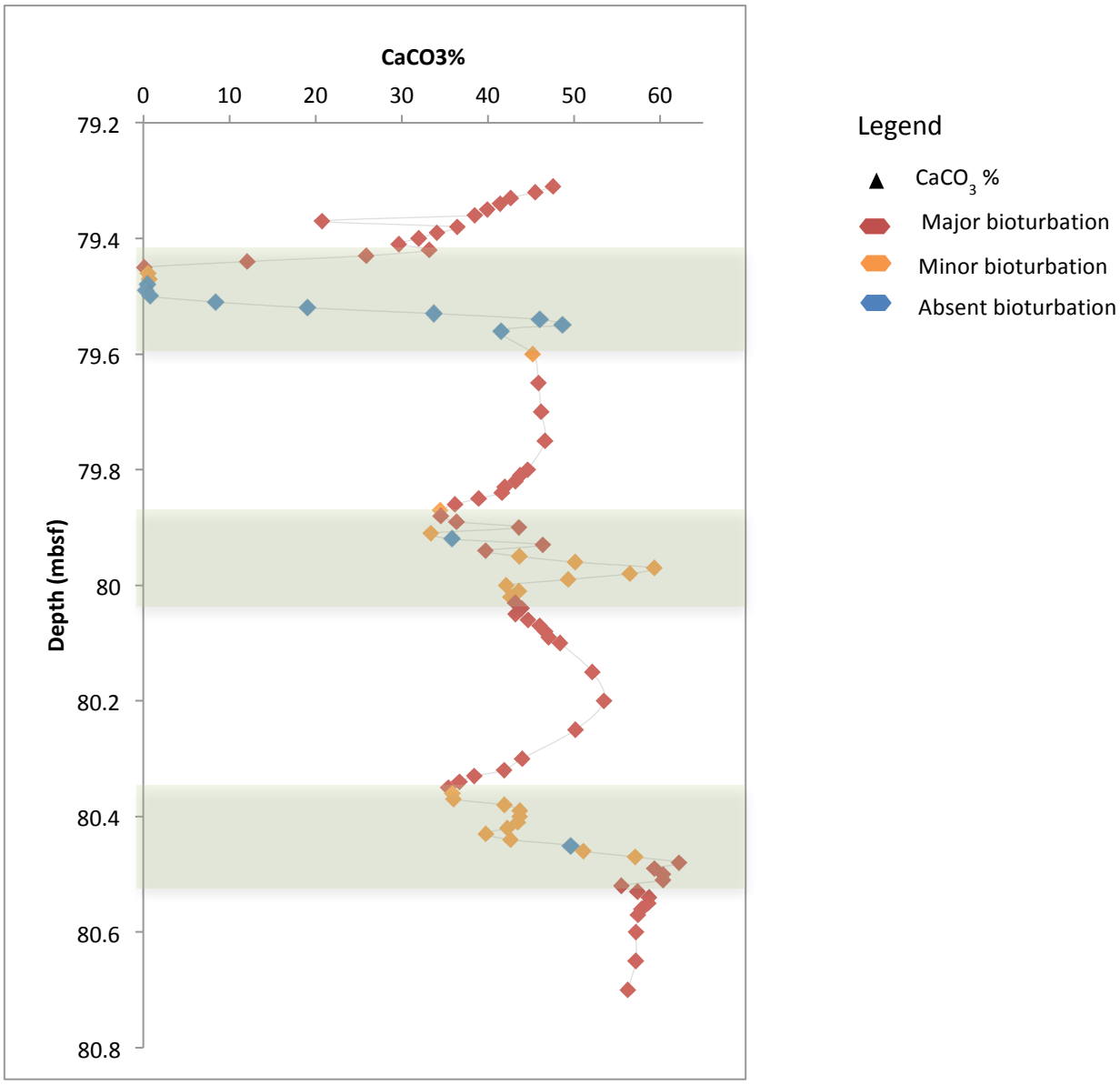

Figure 6: $CaCO_3$ contents plotted against depth (mbsf-refer to Figure 5) for sapropel cycles i-280-i-284 (grey boxes). I-280 has very low/absent percentages of $CaCO_3$ within the sapropel cycle compared to i-282 and i-284 whose $CaCO_3$ contents are not substatially lower than the marls. Symbol colours refer to the degrees of bioturbation within the samples as explained in Figure 5.

TOC and MSA values are also reported on a carbonate free basis because of the large variations in carbonate content and the variable impact of carbonate dilution associated

with this. On a carbonate free basis, i-284 has the highest TOC value with a maximum of 19.4% and an average of 11.8%, while i-280 now records the second highest TOC values with an average of 8.8% and maximum of 15.8% (Figure 5). The middle sapropel still has the lowest TOC values with an average of 7.6% and maximum of 11.5% (Figure 5).

SURFACE AREA RESULTS:

Surface area results obtained with the EGME method range between 513.3m^2g^{-1} to 143.1m^2g^{-1}(Table 1, Figure 7). Marls have an average surface area of 195.3m^2g^{-1} with a maximum of 251.8m^2g^{-1} and a minimum of 143.130m^2g^{-1}, with substantially lower apparent EGME surface areas than sapropels. I-280 records the highest average surface area of 327.8m^2g^{-1} and maximum of 513.3m^2g^{-1}, while both i-282 and i-284 both have similar surface areas ranging between 164.4m^2g^{-1} to 303.5m^2g^{-1}.

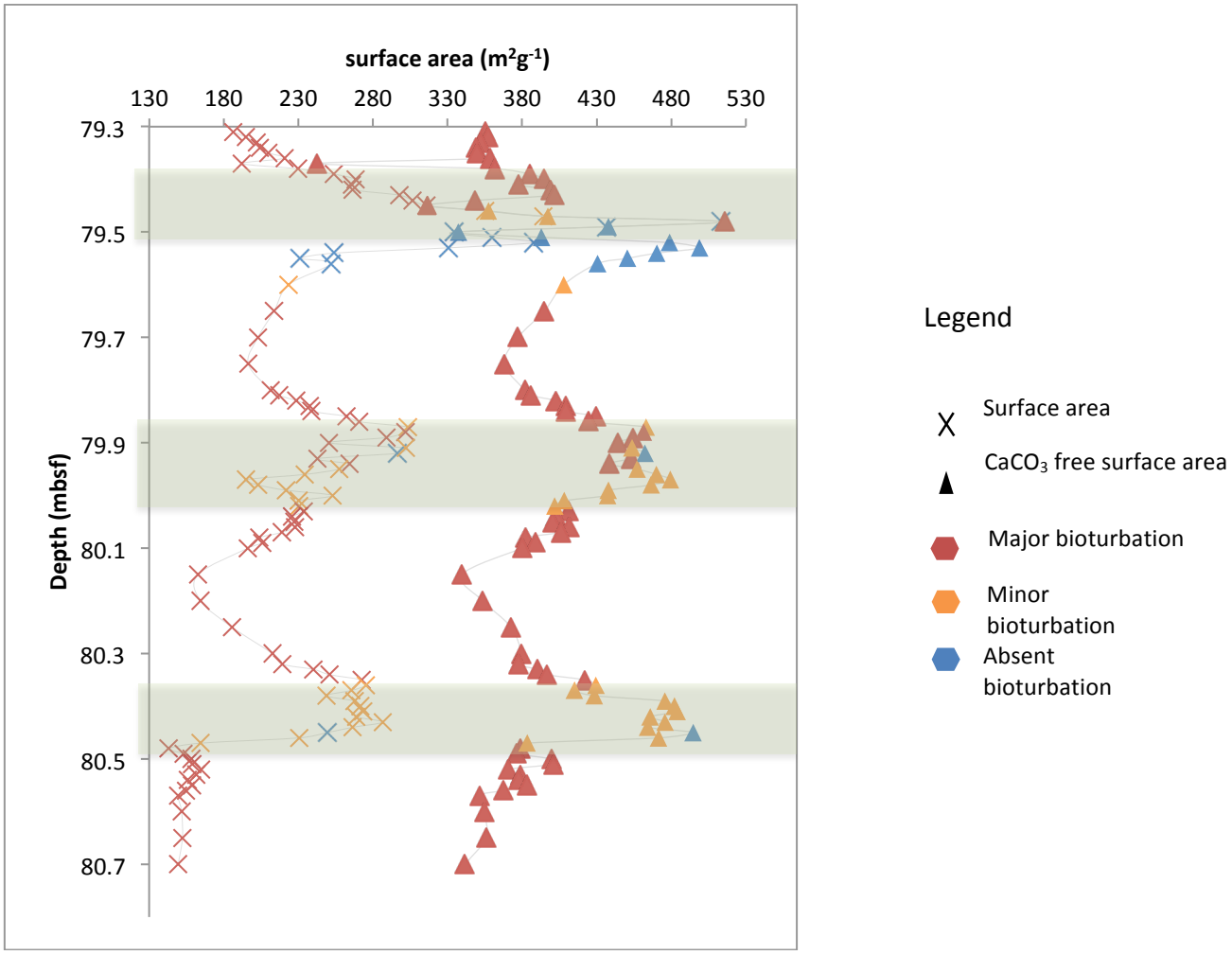

Figure 7: Ethylene Glycol Monoethyl Ether (EGME) measured surface areas and $CaCO_3$ free surface areas with depth (mbsf) of sapropel cycles i-280 – i-284 (grey boxes). Surface areas measured in sapropel cycle i-280 record the highest surface area values and the most variability within a sapropel cycle. I-284 records the highest average surface areas on a carbonate free basis. I-282 records the lowest surface areas and surface areas on a carbonate free basis out of the three sapropel cycles. Symbol colours refer to the degree of bioturbation in which the sample has undergone, as explained in Figure 5.

$CaCO_3$ correction for surface area was also conducted to account for variation in carbonate dilution (Table 1). On a carbonate free basis surface areas increased across all samples, with a maximum range of $516 m^2g^{-1}$ and minimum of $242.5 m^2g^{-1}$. Marls recorded an increased average of $376.4 m^2g^{-1}$. I-280 now records the lowest values for surface area with an average of $409.5 m^2g^{-1}$. I-282 and i-284 record higher surface area averages of $445.3 m^2g^{-1}$ and $493.5 m^2g^{-1}$ respectively (Figure 7).

Interaction between EGME and OM is known to occur (Tiller & Smith 1990), and can result in artificially high mineral surface area estimates within samples. Removal of OM and remeasurement of MSA is required to eliminate the possibility of this occurring in the samples tested. In this instance, a significant reduction in measured surface area was noted after removal of organic matter. The reduction in MSA was strongly correlated with the original TOC of a sample, a higher TOC value corresponded to a higher reduction in surface area from the original (Figure 9). This relationship demonstrates quantitatively significant interaction between EGME and OM, so that the surface areas measured on the untreated samples are substantially higher than the true mineral surface area. Consequently, only MSAs measured after OM removal are used to assess a mineral surface control on OC enrichment in sapropels.

Surface areas measured after OM removal vary between a maximum of 322.5m^2g^{-1} and minimum of 143.41m^2g^{-1} with an average of 210.1m^2g^{-1}(Table 1, figure 8). I-280 recorded the highest surface areas with an average of 240.2 m^2g^{-1}. However i-282 and i-284 record much lower surface area averages of 206.8m^2g^{-1} and 182.6m^2g^{-1} respectively which corresponds closely to the previously measured marl surface are average of 195.3m^2g^{-1}.

Surface area from measured OM-removed sapropel samples now shows no correlation to the TOC (Figure 10). While previous correlations of measured surface area and TOC did reveal strong correlations between the two variables (Figure 11).

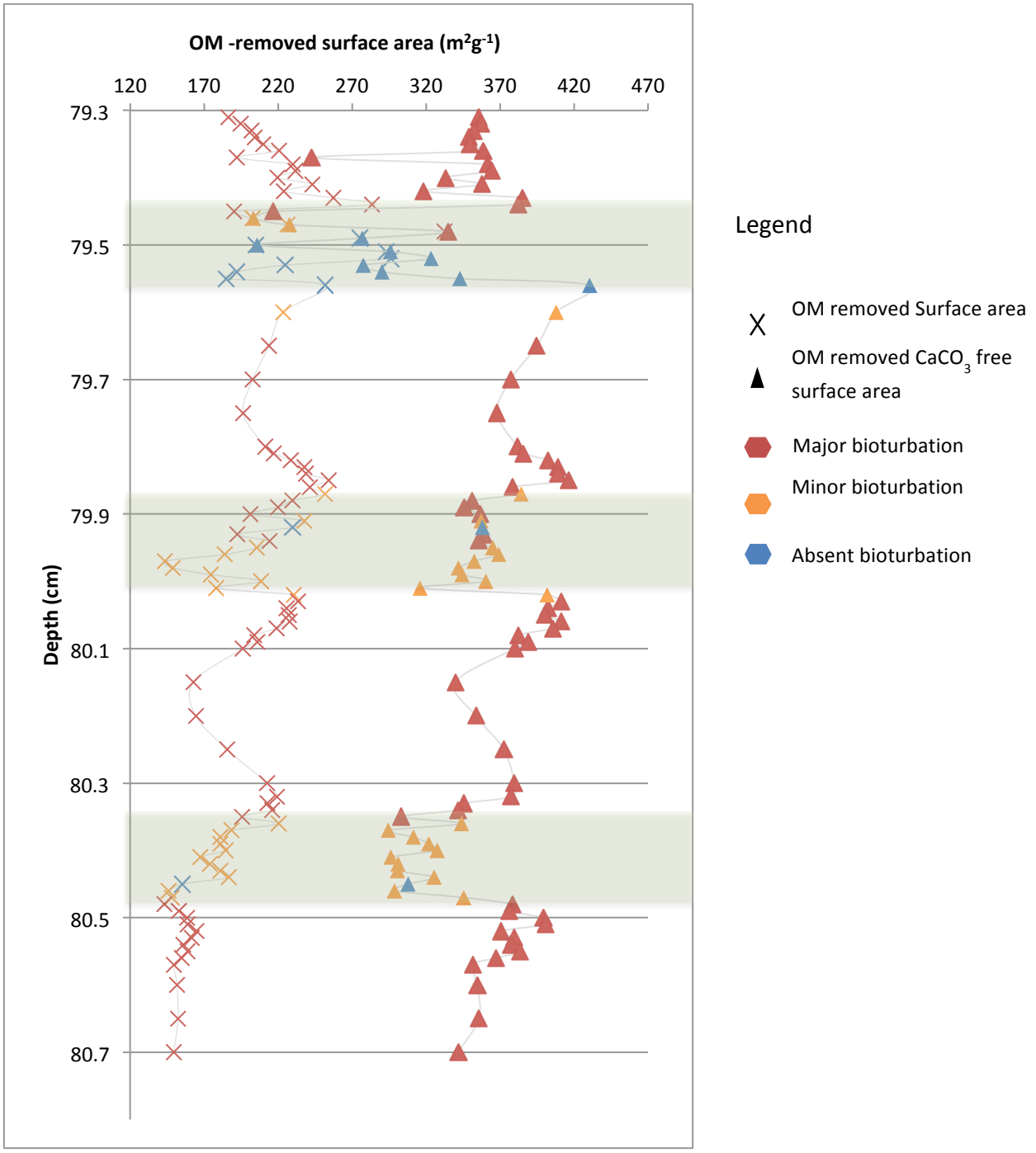

Figure 8: Ethylene Glycol Monoethyl Ether (EGME) measured surface area from samples where organic matter was removed, sapropel cycles i-280 –i-284 (grey boxes), with measured surface areas of marls on $CaCO_3$ free basis with depth (mbsf). From previously calculated surface areas in figure 3 a significant drop in surface area is measured after OM removal. Sapropel surface areas are now indistinguishable from marl surface area, and are shown to decrease when calculated on a carbonate free basis compared to marls. Symbol colours refer to the degree of bioturbation in which the sample has undergone, as explained in Figure 5.

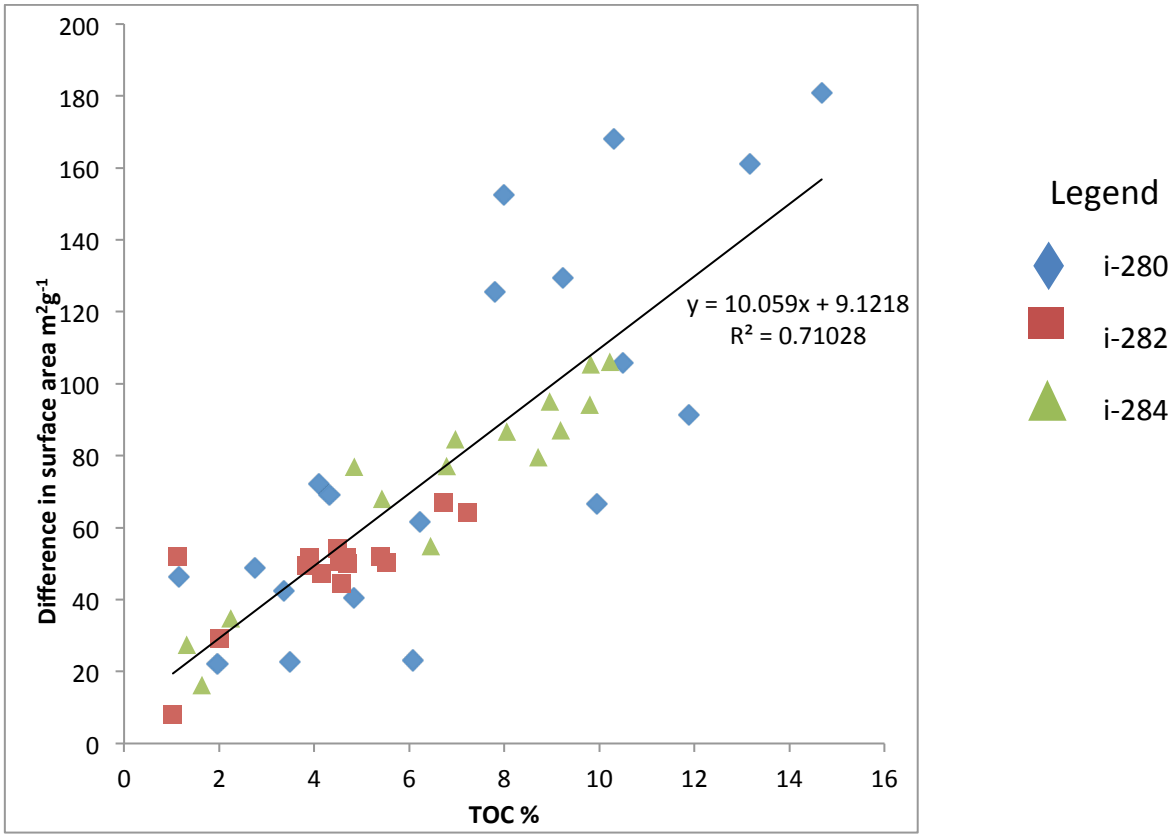

Figure 9: Difference between measured surface area for pre and post organic matter (OM) removed samples for sapropels i-280 (diamond), i-282 (square) and i-284 (triangle) plotted against measured total organic carbon (TOC). A positive relationship exists between the percentage of TOC and magnitude of difference between measured surface areas (MSA). This positive correlation suggests that the method for measuring surface area by Ethylene Glycol Monoethyl Ether (EGME) is flawed and measurement of not only mineral surface area but also OM was taking place at the time of testing. This result voids the hypothesis that MSA assists OM preservation.

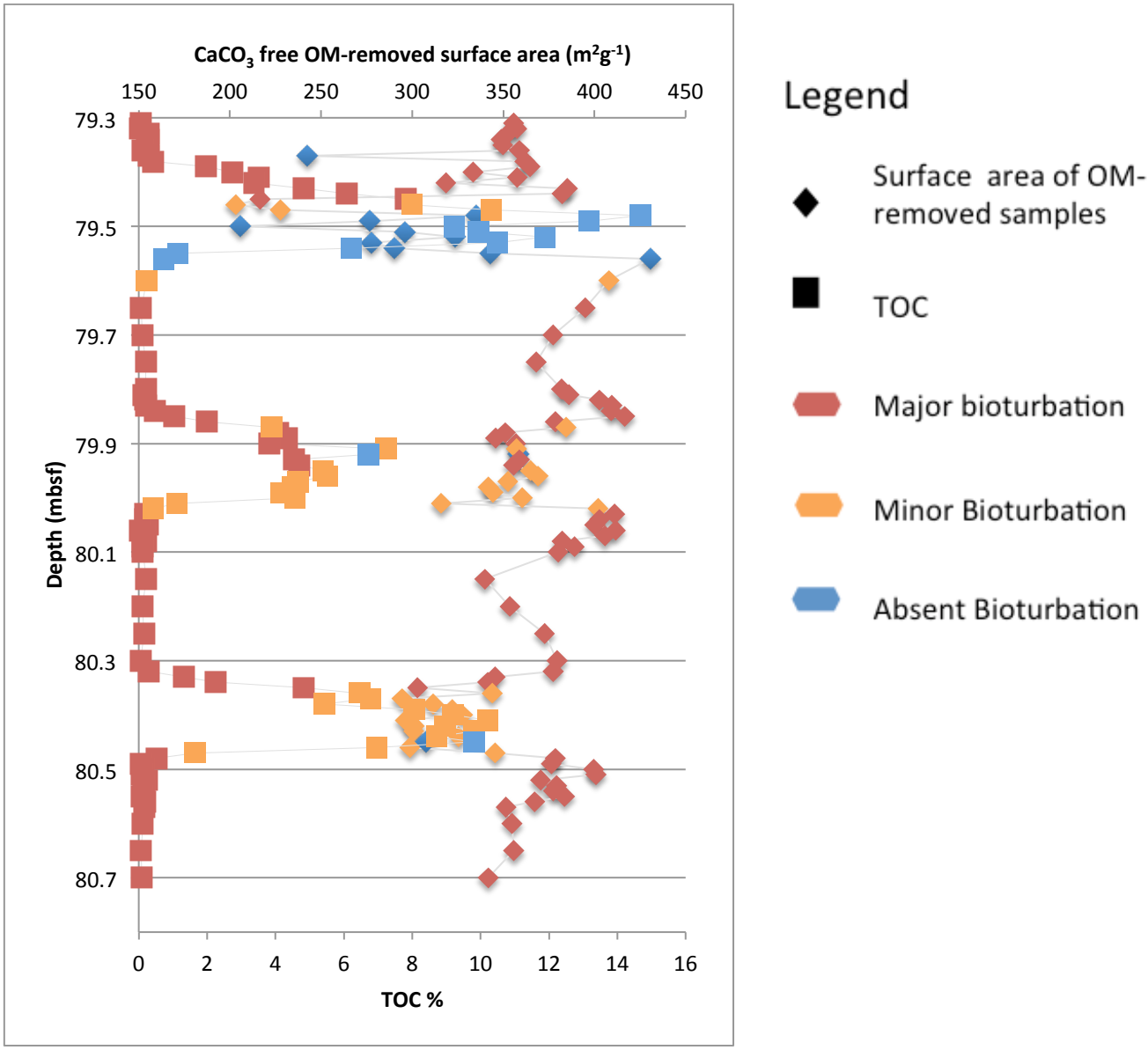

Figure 10: Ethylene Glycol Monoethyl Ether EGME measured surface areas from organic matter (OM) removed sapropels (i-280 to i-284, in the grey boxes) and marls with total organic carbon (TOC) against depth (mbsf). No relationship is recorded between OM-removed samples and TOC, whereas before OM-removal (Figure 11) a clear relationship is seen. Colours represent the varying degrees of bioturbation undergone within the sample as explained in Figure 5.

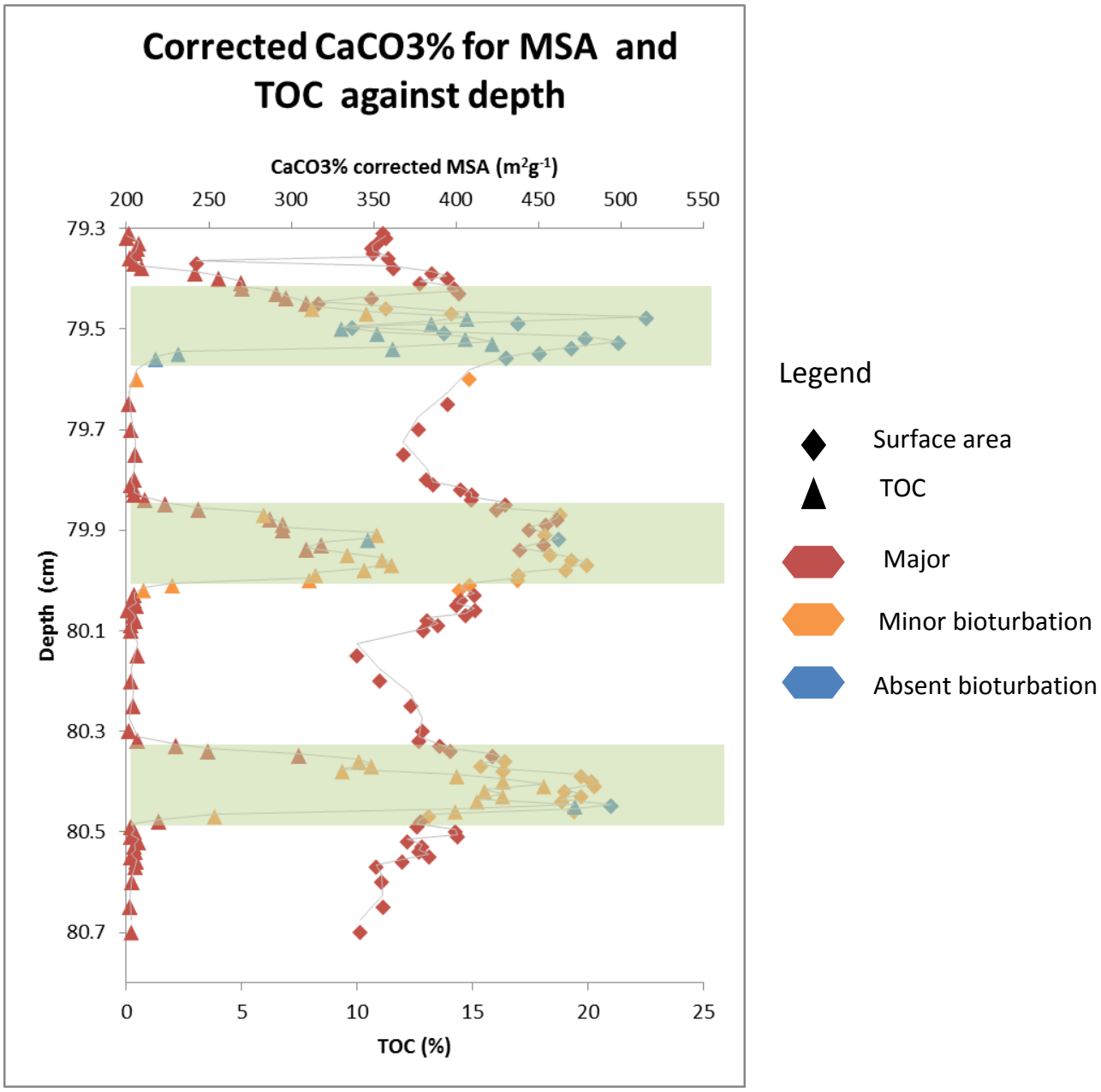

Figure 11: Ethylene Glycol Monoethyl Ether (EGME) measured surface area (MSA) reported on a $CaCO_3$ free basis with total organic carbon against depth (mbsf). Correlation between TOC and MSA shows a strong relationship between the two variables. However from Figure 10 shows that this a 'false positive' relationship. Colours represent the degree of bioturbation undergone by the samples as explained in Figure 5.

From 12 samples chosen within each sapropel cycle, TOC was measured after OM was removed to test for efficiency (Table 2). From this analysis on average 83.2% ± 5.7 of the organic matter was removed from the samples.

Table 2: For sapropels i-280 to i-284, total organic carbon (TOC), TOC contents after organic matter (OM) removal and % of organic carbon (OC) removed after removal for 4 chosen samples within each sapropel.

Sapropel i-cycle	Depth of sample (mbsf)	TOC	TOC after OM was removed	% of OC removed
i-280	79.44-79.45	6.1	0.3	95.6
	79.49-79.5	13.2	3.9	70.4
	79.52-79.53	11.9	1.6	86.3
	79.54-79.55	6.2	1.3	79.5
i-282	79.91-79.92	7.2	1.1	84.2
	79.93-79.94	4.5	0.9	81.2
	79.95-79.96	5.4	0.7	86.8
	79.97-79.98	4.7	0.7	86.0
i-284	80.37-80.38	6.8	1.0	85.3
	80.38-80.39	5.4	1.1	79.0
	80.41-80.42	10.2	1.8	82.0
	80.44-80.45	8.7	1.5	82.6

Measured surface area values from the organic matter removed samples are also reported on a carbonate free basis (figure 8). On a carbonate free basis the recorded surface area values now range between a maximum of 416.5 m^2g^-1 and minimum of 203.1 m^2g^{-1}(table 1). I-282 now records the highest surface areas with a high average of 359.5 m^2g^{-1}. I-280 and i-284 record lower surface area averages at 302.1 m^2g^{-1} and 317.7 m^2g^{-1} respectively.

Clay mineralogy

XRD analysis of the clay fraction shows that kaolinite, illite, chlorite and smectite are present in all 6 samples with no dominant shift in clay mineralogy between marls and sapropels observed (Figure 12). However, palygorskite, a known aeolian sourced clay mineral from the northern borderlands or Africa is found in 3 sapropel samples from i-

284 and one marl (Figure 12). Previous studies have recorded a switch of mineralogy between marls and sapropels and a distinct decrease in aeolian sourced clays during sapropel deposition (Wehausen & Brumsack 1999, Foucault & Melieres 2000). Therefore these results are in contrast and show no prominent switch at site 967.

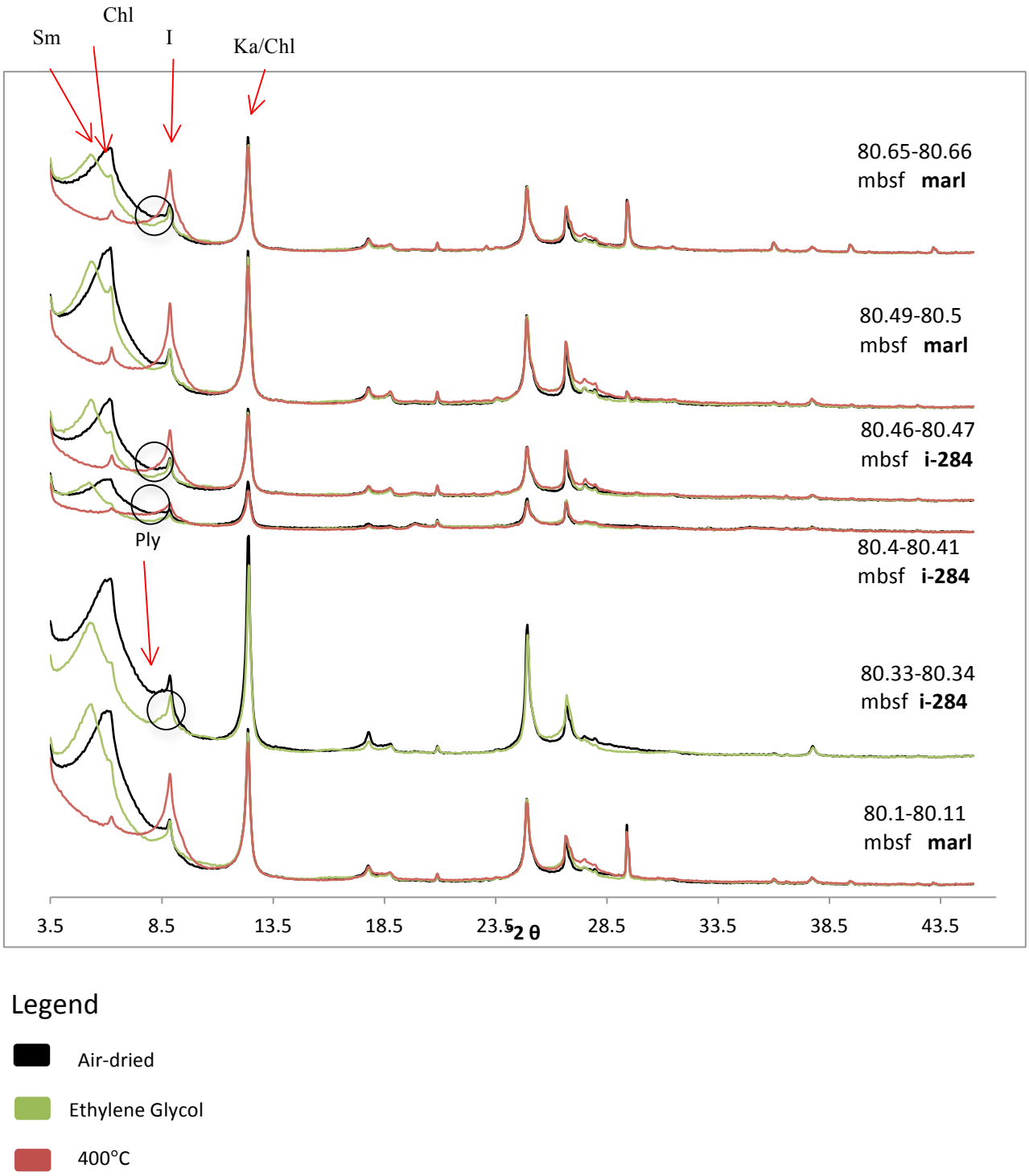

Figure 12: X-ray diffraction patterns of 6 samples ranging from marl to marl through sapropel i-284 show that smectite (Sm), illite (I), kaolinite (Ka) and chlorite (Chl) are present within all samples. However, the palygorskite (Ply) occurs only in 3 sapropel samples and one marl sample highlighted by the black circle. Within the black circles Palygorskite is shown as a slight shoulder off of the illite peak.

Association of OM within the mineral matrix:

SEM BSEI of sapropels identified two distinct patterns of OM association with the mineral matrix within the three studied sapropels (Table 3, Figure 13). OM in i-280 samples 79.44-79.45 mbsf and 79.49-79.50 mbsf is concentrated in OM rich, wavy laminae with an average thickness of 50μm sandwiched between clay and pyrite rich laminae of average thickness of 100μm. The OM rich laminae do not contain significant amounts of detrital minerals such as clays and quartz, conversely the laminae in which detrital clays, quartz and authigenic pyrite are concentrated do not contain appreciable quantites of OM. OM rich laminae is here termed Type I, distinguished from Type II by the segregation from detrital minerals. It is notable that Type I organic matter occurs only in samples characterised by low $CaCO_3$ %. The second type of OM association (Type II), was observed within in all other sapropel samples imaged in i-280, i-282 and i-284. Type II OM association is observed in samples with >30% $CaCO_3$ content, and is characterised by small non-laterally continuous OM-rich laminae of average 50μm length and thickness between 10-20μm and smaller irregular shaped organic-clay aggregates of varying concentrations averaging 20μm in size and gradational boundaries to the surrounding matrix (Figure 14).

Table 3: Total organic carbon (TOC) percentage, CaCO3 percentage, bioturbation status and type of OM association within imaged samples from sapropels i-280 –i-284. Sapropel samples imaged under scanning electron microscope using backscatter electron imagery are distinguished into two types different types of OM association within the mineral matrix, type I and type II. Type I refers to OM within the mineral matrix that is found within thick laminae of average size 50µm. Type II refers to OM present within the mineral matrix in small lamiae size of 50-10µm and as segmented OM in the presence of clays in varying concentrations

Sample	Depth (mbsf)	TOC %	% $CaCO_3$	Bioturbation	Type of OM association
i-280	79.44-79.45	6.1	12	Major	I
	79.49-79.5	13.2	0.3	Absent	I
	79.54-79.55	6.2	46	Absent	II
i-282	79.88-79.89	4.1	34.5	Major	II
	79.91-79.92	7.2	33.4	Minor	II
	79.93-79.94	4.51	46.4	Major	II
i-284	80.37-80.38	6.81	36	Minor	II
	80.41-80.42	10.2	43.5	Minor	II
	80.46-80.47	7	51	Minor	II

The differences in OM viewed in type I and type II could be due to the physical reworking and ingestion of OM by organisms in the process of bitoturbation. Reworking of OM could explain the dispersed nature of OM in the mineral matrix and the association of OM with clay detrital minerals seen within samples displaying Type II association. However, this has been ruled out as the two samples that show type I OM association, 79.44-79.45 mbsf and 79.49-79.50 mbsf, have major and absent bioturbation respectively, and the type of OM does not substantially change with major bioturbation and physical disruption of the Type I OM laminae. Although the OM rich laminae become dirupted as a result of bioturbation, they did not loose their shape and did not become dispersed and mixed with detrital clays as is typical of Type II OM association (Figure 14).

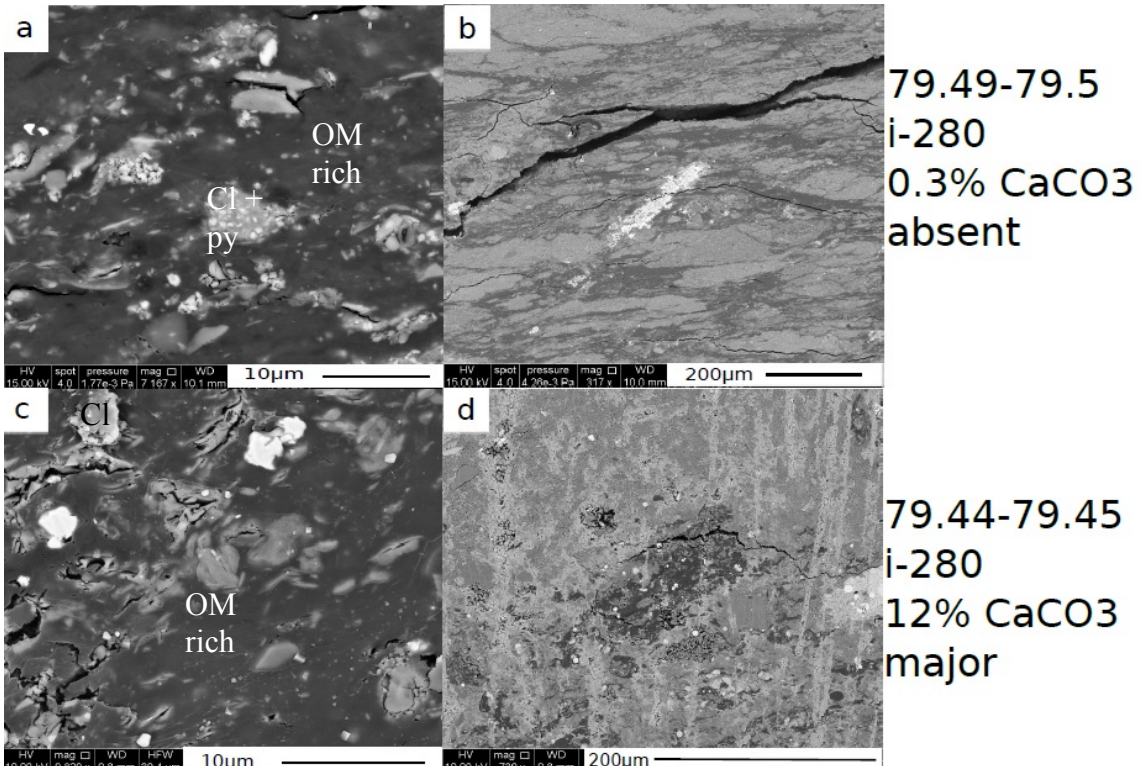

Figure 13: Photo composite showing Type I organic matter (OM) association between two sapropel samples from i-280 of absent and major bioturbation effects. Photo's a and c show association of OM within the mineral matrix. At this scale bioturbation has not reworked the OM with the detrital fraction and Om is similarly discrete in the two samples. At a larger scale however shown in b and d, the laminae evident within b are broken from the reworking by bioturbation in d. The shorthand text on the images implies clays (Cl), clays mixed with pyrite (Cl + py) and organic rich lamine (OM rich).

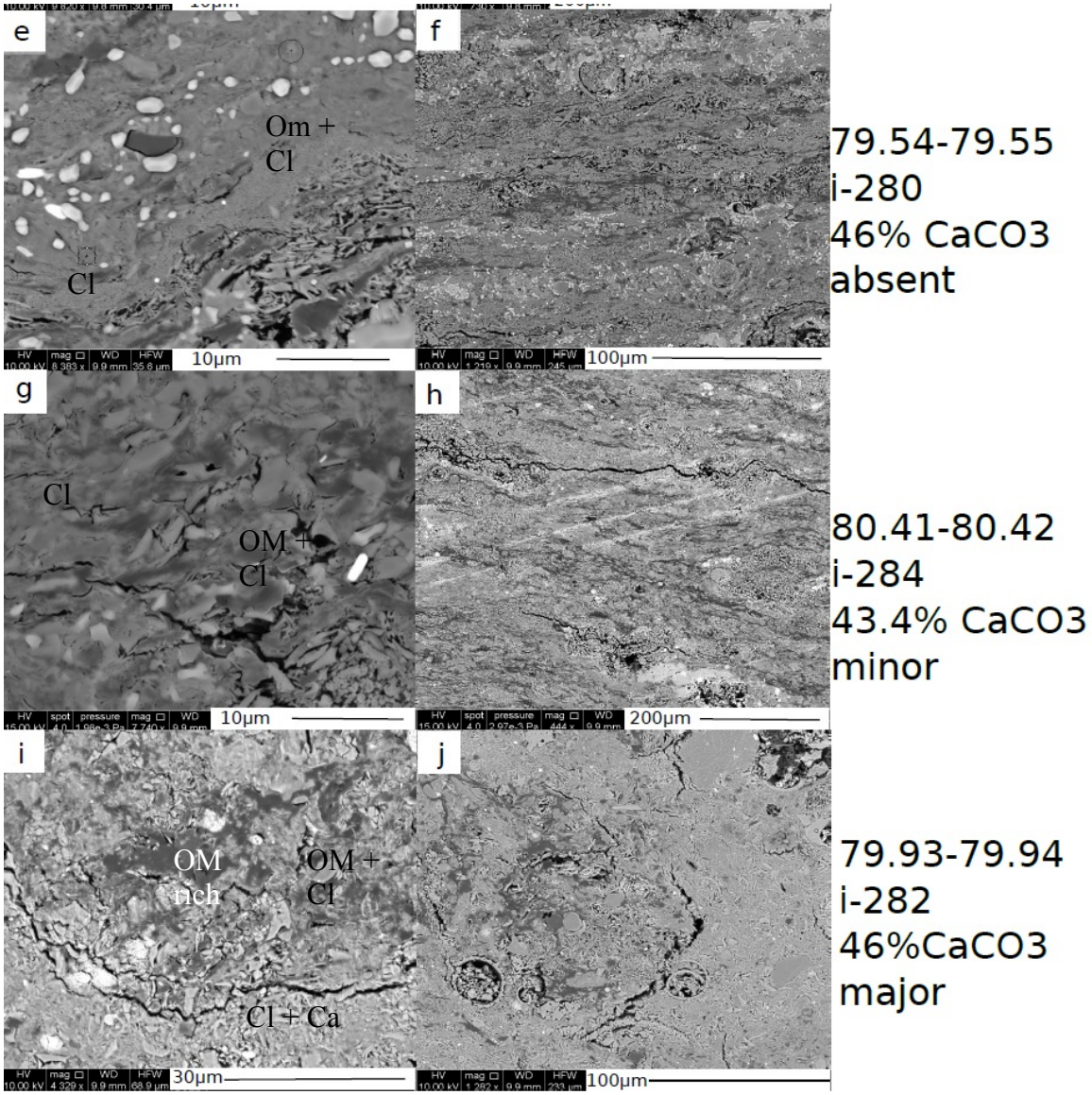

Figure 14: Photo composite of samples from sapropel i-280, i-282 and i-284 placed from lowest to highest degree of bioturbation to show the effect of reworking by bioturbation on organic matter (OM) and the mineral matrix. Photo's e, g and f show close up examples of how Type II OM association within the mineral matrix is displayed in the sapropels. The degree of bioturbation upon these samples shows no disturbance to how they are preserved up close. The OM is associated in small 20-10 µm sized OM-clay aggregates which have disperseved boundaries to the remaining mineral matrix. However some OM rich laminae is present, although this is small (20µm scaled) and occur irregularly. Photos f, g, and j show at a larger scale the effect of bioturbation, with greater disruption in the fabric from f-j with increasing dgerees of bioturbation. The shorthand text on the images implies clays (Cl), clays mixed with organic matter (Cl + OM), clays mixed with carbonate (Cl + C) and organic rich lamine (OM rich).

DISCUSSION

Previous studies by Wehausen and Brumsack (1999) and Foucault and Melieres (2000) have noted a shift in clay mineralogy from marls and sapropels. Where clay types dominating the marl facies and characteristic of aeolian dust from North Africa, are present in lower concentrations within the sapropel sediments, which are dominated by fluvially sourced clays (Wehausen & Brumsack 1999, Foucault & Melieres 2000). However, data gathered during this study, does not show such a switch in clay mineralogy between marls and sapropels. Instead clay mineral such as palygorskite, a clay diagnostic of North African (Saharan) dust, is present in both marls and sapropel samples being identified in three samples from sapropel i-284 and one marl from a marl section above the sapropel (Figure 12). Similarly, previous work at other locations in the EMB (Wehausen & Brumsack 1999, Foucault & Melieres 2000) has shown a cyclical increase in smectite clay in sapropels relative to marls, consistent with a fluvial source for smectite clay. In this context higher smectite abundances within sapropels were expected also at site 967, however, no such shift was observed (Figure 12).

Following clay XRD results from site 967 which show no marked difference between marls and sapropels for smectite content, one possible explanation for this may be found in Nd and Sr isotopic work by Weldeab *et al.* (2002). This study revealed that a dominance in Nile sediments regardless of facies (i.e. marl vs sapropel) existed in the area near site 967, so that minor changes in Aeolian input are masked (Weldeab *et al.* 2002). With little difference in all clays noted from XRD analysis (Figure 12), from site 967, a dominance from a singular source is capable of explaining the non-existent shift present between marls and sapropels.

Similarly this is consistent with high mineral surface area values measured by the EGME method for both the OM-removed sapropel and marl samples (~200m^2g^{-1}, Figure 8). As EGME surface area is particularly sensitive to the presence of smectite, which yields a high surface area (Kennedy *et al.* 2002, Kennedy & Wagner 2011), this result leads us to believe there is a dominant source of smectite to the site. Previous studies (Keil *et al.* 1994, Mayer 1994, Kennedy *et al.* 2002, Kennedy & Wagner 2011), have revealed that a positive correlation between sediment mineral surface area and sediment TOC attributable to a mechanistic relationship in which clay minerals have a preservative effect on OM. Mineral surface area, is dependent on the abundance of weathering derived clay minerals, particularly the concentration of smectite clay (Kennedy *et al.* 2002, Kennedy & Wagner 2011). However, no correlation between MSA and TOC was found at site 967 despite large mineral surface area values (~200m^2g^{-1})(Figure 9 and 10) and an abundance of smectite (Figure 12). This implies that OC enrichment is not dependent upon mineral surface area preservation, within the Mediterranean sapropels studied here.

This result is further supported by SEM images which shows that high TOC samples with low $CaCO_3$ contents do not show associations between the mineral matrix and OC. Both samples 79.44-79.45 and 79.49-79.5 mbsf show a type I OM association (Table 2). With discrete OM rich laminae present between laminae of detrital clays, quartz and authigenic pyrite, there is an absence of any type of organic-clay aggregate found within these samples (Figure 13). This lack of association within the mineral matrix would account for the lack of covariance present between the TOC and surface area (Figure

10). However from SEM images of other samples show a type II OM association (Table 2, Figure 14) where organic-clay aggregate are found in with the mineral matrix. This suggests that there may be a role for clay preservation however, it is not the controlling factor for OC enrichment at this site.

Organic carbon enrichment in sapropels has been widely attributed to improved preservation due to anoxia and increased organic flux due to high productivity (Rohling 1994, Emeis *et al.* 1998, Kemp *et al.* 1999, Passier *et al.* 1999, Nijenhius & De-Lange 2000). Both mechanisms have been studied extensively within the Mediterranean Basin and proved to be relevant with large support from the scientific community. Kemp *et al.* (1999) proposed a model combining both high productivity and anoxia within the water column during the formation of sapropels. Their model describes a switch of seasonal siliceous productivity as indicated by the differences between spring blooms and summer stratified productivity 'fall-dump' events (Kemp *et al.* 1999). Mat-forming rhizosolenid diatoms require straitified conditions and are very sensitive to changes in the water column. The end of summer stratified growing conditions for the mat-forming rhizosolenid diatoms (Kemp *et al.* 1999) results in agitation of the water column and the sudden sedimentation of large quantities of OM and biogenic silica as diatom mats sink to the sediment-water interface.

However, the Mediterranean is a silica poor environment and silica is susceptible to dissolution and often causing very little to be preserved (Nijenhius & De-Lange 2000). However, elevated concentrations of silica have been recorded in some sapropels. Nijenhius and De-Lange (2000) studied sapropel i-280 from 3 sites (964, 967 and 969),

measuring elevated biogenic silica (opal) at 4 w.t.% concentration suggesting an increase in siliceous productivity at the time of formation. Furthermore the $CaCO_3$ concentrations within sapropels are generally lower compared to marls suggesting possible decreases in carbonaceous productivity to increased siliceous productivity.

Lower $CaCO_3$ content (Figure 6) within the samples could be explained by varying degrees of dilution and dissolution. Alternatively they also could represent changes in the dominant productivity type within the water column. However, dilution and dissolution of the $CaCO_3$ can be ruled out for samples with reduction in carbonate contents of greater than 80%. First, dilution would not be able to account for such great reduction in $CaCO_3$ content since it would require a 50 fold increase in non-carbonate detrital materials into the Mediterranean (Weldeab *et al.* 2003) which is unlikely, and no substantial evidence for changes in sedimentation rate between marls and sapropels at this site is present. Furthermore, dissolution of the $CaCO_3$ fraction would require oxidation of OM under anoxic conditions to produce organic acids (Weldeab *et al.* 2003). However, to achieve such a degree of OM oxidation reduction of large amounts of sulphate would be required which in turn would create alkaline waters preventing the dissolution of $CaCO_3$ from proceeding (Weldeab *et al.* 2003). In high productivity settings (i.e. upwelling zones), siliceous rather than carbonaceous secreting organisms are more dominant, with shifts towards lower $CaCO_3$ content in sediments (Nijenhius & De-Lange 2000). This is consistent with the shifts of lower $CaCO_3$ content of sapropels with higher enrichment of OC and Kemp *et al.* (1999) proposed model of diatom productivity with fall-dump cycles.

Furthermore, when examined, Type I OM association shows strong lamination of discrete OM between detrital laminae. Such laminations could represent the disruption of continuous sedimentation (detrital laminae) by the fall-dump event of Kemp *et al.* (1999) (discrete OM rich laminae). In addition to this, the immense decrease of $CaCO_3$ content within these Type I OM samples (79.44-79.45 and 79.49-79.5 mbsf) could represent dominant productivity of diatomaceous mats. The silica tests from the diatom-mats would dissolve in the low silica Mediterranean water (Nijenhius & De-Lange 2000) and concentrate the OM within the laminae observed. Additionally, with large accumulation rates of OM within a single event, the system could become overwhelmed and prevent the breakdown of OM. Passier *et al.* (1999) found that within sapropel i-280 anoxic conditions where present within the photic zone as evidenced by isorenieratene, a biomarker for euxinic water conditions in the photic zone, thereby confirming the presence of anoxic conditions at the time of sapropel formation. In this case clays have no preserving factor within type I OM association, however, it may play a greater role in sediments formed under less productive water columns, as evidenced in samples with higher $CaCO_3$ contents and type II OM association.

Type II OM association where organic-clay aggregates could be interpreted as the product of physical reworking and ingestion of OM through bioturbation. This physical reworking could result in the mixing of detrital clays during bioturbation within previously Type I OM association, creating a change in the physical relationship within the mineral matrix for how OM and clays are associated. However, from Figure 13 and Figure 14 the effect of bioturbation is not visible in how the OM is preserved within the mineral matrix, bioturbation only seems to disrupt the fabric of the OM, as seen from

Type I and Type II samples representing varying degrees of bioturbation. Type II OM association is expressed within samples with greater than 30% $CaCO_3$ content. The organic-clay aggregates expressed within Type II association could merely be the product of the different productivity within the water column at time of formation. If Type I OM association is dominated by siliceous productivity with large fall-dump events and little carbonaceous input then Type II could merely be the symptom of diminished fall-dumps and higher carbonate productivity. With a greater input from carbonate productivity, and a greater mixing of OM and detrital sediments in the water column, from less disruption in sedimentation by strong fall-dump events, greater mixing between OM and clays could have resulted in the organic-clay aggregates observed.

Sapropel formation could therefore be the enrichment of OC by both anoxia and higher productivity rates. From models by both Emeis *et al.* (1998) and Myers (2002) an increase in freshwater to the Mediterranean resulting in a decreased salinity in surface waters would result in the inhibition of circulation within the Mediterranean. Decreased salinity from Emeis *et al.* (1998) model occurs 600-1500 years before the onset of sapropel formation and could be the mode in which nutrients are trapped within the intermediate layer in the Mediterranean. With a decrease in salinity within the surface waters, the Mediterranean production of intermediate water changes location to the Adriatic Sea, where it flows both east over the EMB and west of the Strait of Sicily (Myers 2002). A salinity decrease also inhibits the formation of downward convection of oxygen by the formation of deep waters (Rohling 1994, Emeis *et al.* 1998, Myers 2002). If downward convection was ceased 600-1500 years before sapropel formation,

this would allow for the slow oxygen depletion of bottom waters, creating anoxia in the Mediterranean (Emeis *et al.* 1998). Productivity would thereby increase with increasingly trapped nutrients by the AIW and new circulation scheme (Myers 2002). With stagnation and the increased supply of nutrients, diatomaceous rhizosolenid mats can circulate between nutrient rich deep waters and the higher photic zone (Kemp *et al.* 1999). The death of these diatomaceous rhizosolenid mats at the end of the summer stratified season from strong fall/winter cooling by northerly winds would subsequently create fall-dump events from the rhizosolenid mats and large accumulation rates of OM in a singular event, type I OM association (Kemp *et al.* 1999). However if nutrients trapped weren't sufficient, then only moderate productivity would prevail in the Mediterranean resulting in mixed sedimentation of detrital minerals and OM as it settled to the floor, type II OM association.

CONCLUSION:

In conclusion, mineral surface area preservation by smectite is not the primary control of preservation of OM within the Mediterranean with no strong link between MSA and TOC. However, data generated by SEM imaging supports the model of OC enrichment presented by Kemp *et al.* (1999). With Type I OM association matching the description of 'fall-dump' events generated at the end of the summer stratified season by diatomaceous rhizolsolenid mats. As such, this study provides new evidence supporting the OC enrichment method highlighted by Kemp. The study however questions EGME testing of MSA and how these results are collected. Further study of the sapropels

should be conducted as to determine how different types of productivity (silica or carbonate) govern the preservation of OM within the Mediterranean.

ACKNOWLEDGMENTS

I would like to thank first and foremost my supervisor Stefan Loehr who helped me through this difficult year and teaching me how to be an independent researcher. I would like to thank Tony Hall who provided me with valuable laboratory knowledge and Troy Granger who helped with the collection of data. I would like to thank Claire Kenefick for taking me on a field trip adventure, and valuable help with my thesis. I would also like to thank my fellow members of the Sprigg Geobiology center, especially Martin Kennedy and Lisa Baruch. I wish to thank the Sprigg Geobiology center and the ODP for providing core samples and laboratory facilities. I would like to thank Adelaide Miscroscopy and ASP for providing materials key to the completion of my thesis. I would like to thank Katie Howard for being a great teaching support officer and helping out. Finally I would like to thank Jake MacFarlane for helping with thesis revisions.

REFERENCES

ADAMSON D. A., GASSE F., STREET F. A. & WILLIAMS M. A. J. 1980. Late Quaternary history of the Nile. *Nature* **288**.

ANDERSON J. 1963. An improved pretreatment for mineralogical analysis of samples containing organic matter. *Clays and Clay Minerals* **10**, 380-388.

BENSON R. H., BIED K. R.-E. & BONADUCE G. 1991. An important current reversal (influx) in the Rifian corridor (Morocco) at the Tortonian-Messinian boundary: the end of Tethys Ocean. *Paleoceanography* **6**, 164-192.

BETHOUX J.-P. 1993. mediterranean sapropel formation, dynamic and climatic viewpoints. *Oceanologica Acta* **16**, 127-133.

BOULOUBASSI I., ROLLKOTTER J. & MEYERS P. A. 1999. Origin and transformation of organic matter in Pliocene-Pleistocene Mediterranean sapropels: organic geochemical evidence reviewed. *Marine Geology* **153**, 177-197.

BURDIGE D. J. 2007. Preservation of organic matter in marine sediments: controls, mechanisms, and an imbalance in sediment organic carbon budgets? *Chemical Reviews* **107**, 467-485.

CALVERT S. E., NEILSEN B. & FONTUGNE M. R. 1992. Evidence from nitrogen isotope ratios for enhanced productivity during formation of eastern Mediterranean sapropels. *Nature* **359**.

CHAMLEY H. 1989. *Clay sedimentology* (Vol. 623). Springer-Verlag New York.

CLAUSSEN M., KUBATZKI C., BROVKIN V., GANOPOLSKI A., HOELZMANN P. & PACHUR H. J. 1999. Simulation of an abrupt change in Saharan vegetation in the Mid‐Holocene. *Geophysical Research Letters* **26**, 2037-2040.

CRAMP A. & O'SULLIVAN G. 1999. Neogene Sapropels in the Mediterranean: a review. *Marine Geology* **153**, 11-28.

EMEIS K.-C., SAKAMOTO T., WEHAUSEN R. & BRUMSACK H.-J. 2000. The sapropel record of the eastern Mediterranean Sea—results of Ocean Drilling Program Leg 160. *Palaeogeography, Palaeoclimatology, Palaeoecology* **158**, 371-395.

EMEIS K.-C., SCHULZ H.-M., STRUCK U., SAKAMOTO T., DOOSE H., ERLENKEUSER H., HOWELL M., KROON D. & PATERNE M. 1998. 26. STABLE ISOTOPE AND ALKENONE TEMPERATURE RECORDS OF SAPROPELS FROM SITES 964 AND 967: CONSTRAINING THE PHYSICAL ENVIRONMENT OF SAPROPEL FORMATION IN THE EASTERN MEDITERRANEAN SEA1. *Proc. Ocean Drilling Program, Scientific Results*, pp. 309-331.

EMEIS K. C., ROBERSTON A. H. F. & C R. 1996. Initial Reports Leg 160 Site 967. *Proceedings of the Ocean Drillining Program, Initial Reports* **160**.

EMERSON S. 1985. *Organic carbon preservation in marine sediments.* American Geophysical Union.

FOUCAULT A. & MELIERES F. 2000. Paleoclimatic cyclicity in central Mediterranean Pliocene sediments: the mineralogical signal. *Paleogeography, Paleoclimatology, Paleoecology* **158**, 311-323.

GARCIA-CASTELLANOS D., ESTRADA F., JIMÉNEZ-MUNT I., GORINI C., FERNÁNDEZ M., VERGÉS J. & DE VICENTE R. 2009. Catastrophic flood of the Mediterranean after the Messinian salinity crisis. *Nature* **462**, 778-781.

HEDGES J. I. & KEIL R. G. 1995. Sedimentary organic matter preservation: an assessment and speculative synthesis. *Marine Chemistry* **49**, 81-115.
HILGEN F. 1991. Astronomical calibration of Gauss to Matuyama sapropels in the Mediterranean and implication for the geomagnetic polarity time scale. *Earth and planetary science letters* **104**, 226-244.
IMBRIE J. & IMBRIE J. Z. 1980. Modeling the climatic response to orbital variations. *Science* **207**, 943-953.
KEIL R. G., MONTLUCON D. B., PRAHL F. G. & HEDGES J. I. 1994. Sorptive preservation of labile organic matter in marine sediments. *Nature* **370**.
KEMP A. E., PEARCE R. B., KOIZUMI I., PIKE J. & RANCE S. J. 1999. The role of mat-forming diatoms in the formation of Mediterranean sapropels. *Nature* **398**, 57-61.
KENNEDY M. J., PEVEAR D. R. & HILL R. J. 2002. Mineral surface control of organic carbon in black shale. *Science* **295**.
KENNEDY M. J. & WAGNER T. 2011. Clay mineral continental amplifier for marine carbon sequestration in a greenhouse ocean. *PNAS* **108**.
LOGET N. & VAN DEN DRIESSCHE J. 2006. On the origin of the Strait of Gibraltar. *Sedimentary Geology* **188**, 341-356.
MAYER L. M. 1994. Surface area control of organic carbon accumulation in contiental shelf sediments. *Geochimica et cosmochimica Acta* **58**.
MOORE D. & REYNOLDS R. *JR., 1997. X-ray diffraction and the identification and analysis of clay minerals*. Oxford University.
MULLER P. J. & SUESS E. 1979. Productivity, sedimentation rate, and sedimentary organic matter in oceans-I. Organic carbon preservation. *Deep-Sea Research* **26A**, 1347-1362.
MURAT A. & GOT H. 2000. Organic carbon variations of the eastern Mediterranean Holocene sapropel: a key for understanding formation processes. *Palaeogeography, Palaeoclimatology, Palaeoecology* **158**, 241-257.
MYERS P. G. 2002. Flux-forced simulations of teh paleocirculation of the Mediterranean. *Paleoceanography* **17**.
NIJENHIUS I. A. & DE-LANGE G. J. 2000. Geochemical constraints on Pliocene sapropel formation in the eastern Mediterranean. *Marine Geology* **163**, 41-63.
PASSIER H. F., BOSCH H.-J., NIJENHUIS I. A., LOURENS L. J., BÖTTCHER M. E., LEENDERS A., DAMSTÉ J. S. S., DE LANGE G. J. & LEEUW J. W. 1999. Sulphidic Mediterranean surface waters during Pliocene sapropel formation. *Nature* **397**, 146-149.
PETIT-MARIE N. & RISER J. 1981. Holocene lake deposits and paleoenvironments in Central Sahara, Northeastern Mali. *Palaeogeography, Palaeoclimatology, Palaeoecology* **35**, 45-61.
POPPE L., PASKEVICH V., HATHAWAY J. & BLACKWOOD D. 2001. A laboratory manual for X-ray powder diffraction. *US Geological Survey Open-File Report* **1**, 1-88.
ROBERTSON A. H. 1998. Tectonic significance of the Eratosthenes Seamount: a continental fragment in the process of collision with a subduction zone in the eastern Mediterranean (Ocean Drilling Program Leg 160). *Tectonophysics* **298**, 63-82.
ROHLING E. J. 1994. Review and new aspects concerning the formationof eastern Mediterranean sapropels *Marine Geology* **122**, 1-28.

ROHLING E. J., ABU-ZIED R. H., HAYES J. S. L., HAYES A. & HOOGAKKER B. A. A. 2009. *The marine enviroenment: present and past, in J. C. Woodward (ed.) THe physical Geography of the Mediterranean.* . Oxford University Press, Oxford.

ROHLING E. J., CANE T. R., COOKE S., SPROVIERI M., BOULOUBASSI I., EMEIS K. C., SCIEBEL R., KROON D., JORISSEN F. J., LORRE A. & KEMP A. E. S. 2002. African monsoon variablity during the previous interglacial maximum. *Earth and Planetary Sceince Letters* **202**, 61-75.

ROSSIGNOL-STRICK M. 1982. After the deluge: Mediterranean stagnation and sapropel formation. *Nature* **295**.

ROSSIGNOL-STRICK M. 1983. African monsoons, an immediate climate response to orbital insolation. *Nature* **304**.

ROSSIGNOL-STRICK M. 1985. Mediterranean Quanternary sapropels, an immediate respone of the African monsoon variation of insolation. *Paleogeography, Paleoclimatology, Paleoecology* **49**, 237-263.

SHERROD L., DUNN G., PETERSON G. & KOLBERG R. 2002. Inorganic carbon analysis by modified pressure-calcimeter method. *Soil Science Society of America Journal* **66**, 299-305.

STANELY D. J. & WINGERATH J. G. 1996. Clay mineral distributions to interpret Nile cell provenance and Dispersal. *Journal of Coastal Research* **12**, 911-929.

STRUCK U., EMEIS K.-C., VOB M., KROM M. D. & RAU G. H. 2001. Biological productivity during sapropel S5 formation in the Eastern Mediterranean Sea: Evdience of satble isotopes of nitrogen and carbon. *Geochimica et cosmochimica Acta* **65**, 3249-3266.

TILLER K. & SMITH L. H. 1990. Limitations of EGME retention to estimate the surface area of soils. *Soil Research* **28**, 1-26.

TYSON R. 2005. The" productivity versus preservation" controversy: cause, flaws, and resolution. *SPECIAL PUBLICATION-SEPM* **82**, 17.

WEHAUSEN R. & BRUMSACK H.-J. 1999. cyclic variations in the chemical composition of eastern Meditrranean Pliocene sediments: a key for understanding sapropel formation. *Marine Geology* **153**, 161-176.

WELDEAB S., EMEIS K.-C., HEMLEBEN C., SCHMIEDL G. & SCHULZ H. 2003. Spatial productivity variations during formation of sapropels S5 and S6 in the Meditterranean Sea: evidence from BA contents. *Palaeogeography, Palaeoclimatology, Palaeoecology* **191**, 169-190.

WELDEAB S., EMEIS K.-C., HEMLEBEN C., VENNEMANN T. W. & SCHULZ H. 2002. Sr and Nd composition of Late Pleistocene sapropels and nonsapropelic sediments from the Eastern Mediterranean Sea: implication for detrital influx and climatic conditions in the source area. *Geochimica et cosmochimica Acta* **66**, 3585-3598.

APPENDIX A:

STANDARD PROCEDURE FOR EGME SURFACE AREA MEASUREMENTS: Adapted from Tiller and Smith (1990)

Calcium exchange:

This step is required to ensure that the same cation (Ca) is on the exchange sites of all samples.

Step 1: Weigh 1.1 g of sample into a 50 ml centrifuge tube

Step 2: Add 15 ml of 1 M calcium chloride solution to each sample

Step 3: Place samples on end-over-end shaker for 60 minutes

Step 4: Remove samples from shaker and leave to settle overnight

Step 5: Fill up to 50 ml mark with deionized water

Step 6: Centrifuge samples for 10 minutes at 3000 rpm

Step 7: Pour off the supernatant, be careful not to loose any sample

Step 8: Add 50 ml deionized water to each sample, shake until all sample is suspended

Step 9: Centrifuge samples for 10 minutes at 3000 rpm

Step 10: Pour off supernatant

Step 11: Repeat steps 7-9 once

Step 12: Dry samples in oven at 40°C until dry

Step 13: Once dry, homogenize each sample in agate mortar and pestle, return to centrifuge tubes

Step 14: Store dried samples in oven or desiccator until weighed out for EGME analysis

EGME analysis:

Step 1: Mark sample names on glass vials and plastic caps using a diamond pen

Step 2: Record weight of the marked glass vials and caps using analytical balance to 5 decimal places

Step 3: Weigh 1 g of oven dried, Ca-exchanged sample into the glass vials

Step 4: Place uncapped vials with samples into oven (110^{o}C) for 48 hours to remove all sorbed water

Step 5: Remove vials from oven and cap with the corresponding caps, as quickly as

possible to avoid moisture absorption

IMPORTANT: Wear the white gloves under the nitrile gloves to avoid burning your fingers

Step 6: Leave to cool in desiccator

Step 7: Record the weight of the capped glass vials containing the dry samples

Step 8: Place the vials into the plastic trays containing cardboard dividers – this will make it easier to place and remove the vials into the vacuum chamber

> IMPORTANT: Remember to include 6 replicates of each of the standard clays, Ca-exchanged and oven dried like the samples.

Step 9: Place 200g granular $CaCl_2$ and 40 ml EGME, in separate containers, into the sealed vacuum chamber

Step 10: In the fume hood, add 1 ml of EGME to each sample

Step 11: Place the uncapped vials containing the slurries in the sealed vacuum chamber and evacuate the chamber using the vacuum pump for 10 minutes – check that the vacuum chamber door is properly sealed and that the vacuum is increasing

Step 12: Leave the samples until they all look dry (8-10 days, depending on mineralogy)

Step 13: Replenish the EGME and replace the CaCl2 in the vacuum chamber every few days. This is best done when the samples are removed for weighing. Evacuate the chamber again after you are done – pump for 10 minutes

IMPORTANT: Cap the vials as soon as you remove them from the vacuum chamber to minimize the amount of water that the samples absorb during the weighing process. Get someone to help you if you have a large number of samples, this will speed up the capping.

Step 14: Once the samples have dried weigh them every two days until they have reached a constant weight. This can take up to two weeks.

APPENDIX B: INORGANIC CARBON

Pressure Calcimeter: method adapted from Sherrod *et al.* (2002)
Normalized to the standards and blanks run in sync with the test to a polynomial equation trendline.
Step 1: Cut micro-centrifuge tubes just above the 1.0ml mark.
Step 2: Add 5 ml 4 M HCl/3% $FeCl_2$ solution to each glass vial.
Step 3: Weigh out 200mg of each sample into a cut micro-centrifuge tube and place this into a glass vial containing HCl acid. Make sure that the sample does not come into contact with the acid.
Step 4: Weigh out 7 $CaCO_3$ standards and place into vials containing acid. $CaCO_3$ standard weights: 200mg, 150mg, 100mg, 75mg, 50mg, 25mg and 10mg
Step 5: Cap all vials with a rubber stopper and a foil cap, and then crimp the foil using the hand crimper.
Step 6: Once all samples and standards to be tested are capped shake each vial vigorously to ensure that all of the samples reacts with the acid.
Step 7: Leave the vials sitting for half an hour, shaking them once more at the 15 min mark
Step 8: Attach the hose and needle to the manometer
Step 9: Tear out the center of the aluminium cap on the first vial, pierce the rubber cap with the needle and record the maximum pressure vial. Repeat for all vials.
Step 10: The weight and pressure of the standards and pressure recorded in each sample is then used to calculate the equivalent mass of CaCO3 in each sample. This value needs to be normalized to the exact mass of sample weighed into each centrifuge tube. This is most easily done in excel.
Step 11: Convert %CaCO3 in each sample into % IC
To make the 4M HCl/3% $FeCl_2$: to prepare acid reagent mix 330 ml of concentrated (37%; 36.46 M) HCl with about 500 ml of water in a 1 L volumetric flask. Add 30 g ferrous chloride and dilute to total volume of 1 L.

APPENDIX C:

TOTAL CARBON MEASUREMENT USING A PERKIN-ELMER CHN ANALYSER

Total Carbon is obtained through the use of a Perkin-Elmer CHN analyser.
Step 1: The combustion tube temperature should be 975°C and the reduction tube temperature at 640°C.
Step 2: To calibrate and warm the machine start with the procedure of loading 3 blanks (just the tin foil capsules rolled into a square), 1 $CaCO_3$ (at 3-7mg), 1 blank, 1 $CaCO_3$, 1 blank, 3 S1 standards at 4mg, 1 S2 sample and 1 $CaCO_3$ sample.
Step 3: The $CaCO_3$ should not differ from 12% carbon by more than ±0.1 %. Check that this is right before starting your samples, go by the last $CaCO_3$ run.
Step 4: Run 5 samples with a $CaCO_3$ for a check sample afterwards. Do this for all you samples.
Step 5: Turn the gas saver on at the end of the day and lock up.

APPENDIX D:

SEM: USING THE FEI QUANTA 450

Step1: To prepare the sample for SEM imaging to start you need to subsample your sample into 0.5cm square. The sample then needs to be orientated onto an SEM stand with the bedding plane facing upwards so that the bedding structure can be imaged, and then glue this down using araldite.
Step 2: To flatten and even the sample, first even the sample by using a coarse sandpaper to cut down on the initial unsmooth surface. Next use a finer sandpaper to remove the mechanical appearance of the first sanding.
Step 3: Next to shine and polish the sample further and to remove any contamination or mechanical features imposed on the sample from sandpaper grinding an ion mill, Fishione 1060 SEM mill, is used at a setting for 8 hours.
Step 4: To keep the sample from charging in the FEI Quanta 450 a coat of platinum using the Cressington 208 HR high resolution sputter coater, at 5µm, is needed.
Step 5: Using the FEI Quanta 450, high resolution field emission scanning electron microscope, collect and note different features within each sample and the composition of these features.

APPENDIX E:

CLAY SEPARATION:

Step 1: Weigh out 100mg of sample into 10ml centrifuge tubes.
Step 2: Calcium chloride exchange the samples by adding 5ml of 1mol CaCl solution to each centrifuge tube and shaking the sample vigorously then leave for 30mins.
Step 3: Clean metal slides and XRD sample slides (flat ones). Then write on the dull side of the metal slide the sample number and on the side of the XRD slide.
Step 4: After 30 mins, dilute the centrifuge tubes to 10ml with DI water. And centrifuge them for 15mins at 2000rpm. Pour off the solvent.
Step 5: Rinse sample thrice with DI water.
Step 6: Fill samples with DI water to the 9ml mark and then use the ultra sonic machine set to 30% for a minute.
Note: Make sure to wear ear protection for the ultra sonic as it is loud.
Step 7: Repeat step 6 for all samples.
Note: If you notice the samples starting to settle too quickly you will need to rinse the sample again, before redoing step 6 onwards.
Step 8: Shake the samples well and place within the Eppendorf Centrifuge machine for 4 minutes at 900rpm.
Note: This is for a temperature sample of 25°C, if the samples are at another temperature the time for centrifuging may change.
Step 9: Pipette from the middle of the centrifuge tube the fine fraction of suspended matter onto a silicon slide and dry in the oven at 40°C for 2 hours.
Step 10: Place samples within the Bruker D8 XRD with the method set to clay method.

APPENDIX F:

CLAY IDENTIFICATION:

Ethylene Glycol Treatment: Poppe *et al.* (2001)

To help with the identification of swelling clays, Ethylene Glycol is mixed with the sample already prepared for X-ray diffraction, from the clay separation method above, and used to determine the clays present within the sample. It is a comparative tool.
Step1: Onto the prepared slides drop a single drop, or two if needed to cover and absorb to the surface of the slide and the clay minerals. Make sure it is absorbed to the entire surface of the sample.
Step 2: Place and run the sample in the Bruker D8 XRD with the clay method.

Heat Treatment: Poppe *et al.* (2001)

To further identify the clay's present within the sample, heating of the clay samples can allow for a more accurate assessment on the identification of the clay minerals present. Depending on the mineral species at a certain temperature their structure may collapse due to dehydration or destruction. Heating may also bring changes to the spacing of the crystal structure and therefore the diffraction pattern that is measured.
Step 1: Heat the sample to 400°C in an oven or furnace for at least 30 minutes. Be careful removing and placing the samples in the oven/furnace as you could burn yourself. Use appropriate personal protective equipment and tongs to remove/place sample within oven/furnace.
Step 2: Reanalyse the sample in the Bruker D8 XRD set to the clay method.
Step 3: Based on the Poppe *et al.* (2001) clay mineral identification flow diagram identify the minerals present in the sample.
Step 4: Reheat the sample to 550°C for a minimum of 30 minutes.
Step 5: Reanalyse the sample in the Bruker D8 XRD set to the clay method.
Step 6: Based on Poppe *et al.* (2001) clay mineral identification flow diagram and the Ethylene Glycol and 400°C heat treatment as comparisons reanalyse and reassess the mineral species present within the sample.

APPENDIX G:

CLAY PURIFICATION FOR XRD ANALYSIS: ADAPTED FROM THE METHODS PRESENTED IN POPPE *ET AL.* (2001)

For a better quantitative test to identify the clay minerals first the removal of carbonates (inorganic matter) and removal of organic matter is needed. Organic matter can obscure the diffraction maxima of mineral species and removal of the organics can therefore be used to better identify the mineral species present.

Carbonate Removal:
Step 1: Place 1 g of sample in a 50 ml centrifuge vial
Step 2: Add 10 ml of 1 M sodium acetate/acetic acid buffer
Step 3: Loosely screw on cap and place in water bath at 90 ^{o}C
Step 4: Keep a close eye on the samples, if reacting too vigorously remove to cold water bath until reaction has slowed.
Step 5: As soon as effervescence stops, remove sample from hot water bath
Step 6: Fill up tube to 50 ml with DIW
Step 7: Centrifuge for 5 minutes at 3000 rpm and discard supernatant
Step 8: Repeat steps 2 to 7 twice (keep in hot water bath for 30 minutes during repeats)
Step 9: Fill to 50 ml with DIW, cap and shake sample well
Step 10: Centrifuge for 5 minutes at 3000 rpm, discard supernatant
Step 11: Repeat rinse in DIW twice (three DIW rinses total)
Note: If you are to leave the sample overnight leave the sample sitting in DIW.
Solution for 1M sodium acetate – acetic acid buffer with a pH of 5:
To make up a 1M sodium acetate – acetic acid buffer with a pH of 5 dissolve 136 g of sodium acetate trihydrate ($CH_3COONa \cdot 3H_2O$) in about 900 mL deionized water, then add 45 mL glacial acetic acid and bring the total volume of the solution to 1000 mL by adding deionized water.

Organic Matter Removal:
NOTE: The samples should be carbonate free before OM removal. If the sample contains carbonates, make sure you complete the carbonate removal procedure before proceeding.
Step 1: Adjust the required amount of sodium hypochlorite bleach to a pH of 9.5 using 4M HCl. Use a pH meter as you add the 4M HCl as this will allow you to accurately adjust the formula to the right pH.
NOTE: This needs to be done in the fume hood as it releases a dangerous gas, and should be done on the day that the solution will be used as the resulting solution is not stable. Use a calibrated pH electrode.
Step 2: Dispense 10 ml of the pH-adjusted bleach into each centrifuge vial
Step 3: Loosely cap vials, place vials in a plastic rack and place in a 90 ^{o}C water bath for 15 minutes
Step4: Remove vials from bath, fill to 50 ml with DIW
Step 5: Centrifuge for 5 minutes at 3000 rpm
Step 6: Discard supernatant

Step 7: Repeat steps 2 to 6 until samples no longer react upon addition of bleach and have changed colour to light grey, brown or reddish, indicating complete removal of OM. This usually requires 1-3 repeats.
Step 8: After the last bleach repeat, rinse sample in DIW once more.
Step 9: Centrifuge for 5 minutes at 3000 rpm and discard supernatant
Step 10: Fill to 50 ml with DIW, cap and shake sample well
Step 11: Centrifuge for 5 minutes at 3000 rpm, discard supernatant
Step 12: Repeat rinse in DIW twice (three DIW rinses total)
Note: If you are to leave these samples overnight leave the samples in DIW.

Clay fraction separation <2mm

Step 1: Using the ultra sonic machine to a setting of 30% for 30 seconds, ultra sonic each sample.
Note: Make sure the sides of the container don't touch the tip.
Step 2: Centrifuge for 4 minutes at 900rpm
Step 3: Pour off the supernatant (it should be cloudy) into a beaker labelled with the sample name.
Step 4: Repeat steps 1 to 3 until the supernatant is clear.
Step 5: Place a teaspoon of CaCl2 in each beaker and cover before leaving them to settle for a few days.
Step 6: Vacuum clear supernatant from settled contents in beakers, making sure to not suck any of material away.
Step 7: Pour material into the centrifuge tubes and spin at 3000rpm for 20 minutes.
Step 8: discard the supernatant (it should be clear).
Step 9: Repeat steps 7 and 8 until all material has been transferred from the beakers to the centrifuge tubes. The final portion of the material will need to be washed from the beakers with DIW.
Step 10: Add 10mL of CaCl2 solution to each sample and shake with the vortex mixer. Then fill to the 50ml mark with DIW water.
Step 11: Centrifuge for 10 minutes at 3000rpm. Then discard supernatant.
Step 12: Rinse each sample with DIW for 10 minutes at 3000rpm. Leave the collected material in a centrifuge tube and oven dry at 60°C.